

Division - Soil in Space and Time | Commission - Soil Genesis and Morphology

Genesis and micropedology of soils at Serra do Divisor and Moa river floodplain, northwestern Acre, Brazilian Amazonia

Bruno Araujo Furtado de Mendonça^{(1)*} , **Carlos Ernesto Gonçalves Reynaud Schaefer⁽²⁾** , **Elpídio Inácio Fernandes-Filho⁽²⁾** , **Felipe Nogueira Bello Simas⁽³⁾** , and **Eufran Ferreira do Amaral⁽⁴⁾** 

⁽¹⁾ Universidade Federal Rural do Rio de Janeiro, Instituto de Florestas, Seropédica, Rio de Janeiro, Brasil.

⁽²⁾ Universidade Federal de Viçosa, Departamento de Solos, Viçosa, Minas Gerais, Brasil.

⁽³⁾ Universidade Federal de Viçosa, Departamento de Educação, Viçosa, Minas Gerais, Brasil.

⁽⁴⁾ Empresa Brasileira de Pesquisa Agropecuária, Embrapa Acre, Centro de Pesquisa Agroflorestal do Acre, Rio Branco, Acre, Brasil.

ABSTRACT: The northwestern part of the Acre State (Brazil) possesses singular soils in Brazilian Amazonia, but have been very little studied. This study aimed to discuss the genesis and some micropedological aspects of the soils from Serra do Divisor and adjacent floodplain soils of the Moa river, to enhance the knowledge on their formation. A toposequence of soils ranging from the uppermost part of sub-Andean Serra do Divisor to the Alluvial soils of Moa river floodplain was studied, regarding chemical, physical, mineralogical, and micromorphological attributes. The parent material of the Serra do Divisor is basically quartzose sandstone, and the soils along the toposequence were classified as Typic Haplorthods (P1), Spodic Quartzipsamment (P2), Lithic Quartzipsamment (P3), and Lithic Quartzipsamment (P4). Along the Moa river floodplain, we also identified and collected, Typic Udifluent (P5), Typic Kandiuult (P6), Typic Kandiuult (P7), and Arenic Plinthic Kandiuult (P8). The Serra do Divisor soils have very low fertility, high acidity, and low cation exchange capacities, presenting a coarse sandy texture, even shallow pedons. The X-ray diffraction analysis of these soils indicates the predominance of kaolinite, with traces of quartz and gibbsite. The shallow mountain Podzols on sandstone have an expressive accumulation of organic material in surface horizons, with evidence of ferrihydrite and imogolite in the subsurface. At the Moa river floodplain, all soils are originated from recent sediments (Cenozoic), which have a geological source upstream. Varying sedimentary layers are key aspects influencing soil genesis. Those soils have evidence of 2:1 clays with hydroxyl-Al interlayers in subsurface horizons. The Serra do Divisor steep landforms and the coarse texture of the soils promote good drainage and favor leaching and chemical impoverishment. Kaolinite and gibbsite were formed by severe leaching and there are evidences of in situ neoformation of gibbsite by extreme Si losses. All studied soils have some peculiarities such as high accumulation of organic material or 2:1 clay minerals. Most investigated soils were affected by colluvial, reworking, mass movements or a strong variation on sedimentation.

Keywords: pedogenesis, soil mineralogy, Amazon soils, organic materials, South America.

*** Corresponding author:**

E-mail: brunoafmendonca@gmail.com

Received: March 05, 2020

Approved: June 03, 2020

How to cite: Mendonça BAF, Schaefer CEGR, Fernandes-Filho EI, Simas FNB, Amaral EF. Genesis and micropedology of soils at Serra do Divisor and Moa river floodplain, northwestern Acre, Brazilian Amazonia. Rev Bras Cienc Solo. 2020;44:e0200038. <https://doi.org/10.36783/18069657rbc20200038>

Copyright: This is an open-access article distributed under the terms of the Creative Commons Attribution License, which permits unrestricted use, distribution, and reproduction in any medium, provided that the original author and source are credited.



INTRODUCTION

The northwestern of the Acre State (Brazil) possesses unique, poorly studied pedo-environments in the Brazilian Amazonia. The region is directly associated with the presence of first Andean folded/faulted elevations, under a neotectonic regime. Some peculiar aspects are observed in the formation of these soils, with strong contrasts with lowland Amazon soils (Carvalho et al., 1977). The main physiographic feature in this region is the Serra do Divisor mountain range, reaching 700 m a.s.l., consisting predominantly of Cretaceous sandstones (Moura and Wanderley, 1938; Carvalho et al., 1977).

The Amazonian tropical rainforest is the main vegetation type of this region, developing on sandy soils under an equatorial climatic regime. The combination of humid tropical conditions and a sandy, nutrient-poor substrates could favor the development of illuviation process leading to organic subsurface layers and podzolization, with downward migration of Al/Fe compounds, complexed by organic matter, and subsequent accumulation of amorphous constituent, forming spodic horizon (Lundström et al., 2000; Schaetzl and Anderson, 2005; Soil Survey Staff, 2014a).

Podzolization can be explained by two major processes: (1) formation and downward transport of the organometallic complexes with Al and Fe; (2) weathering of silicates followed by Al and Si translocation, as inorganic forms, or imogolite type materials (Farmer et al., 1980; Anderson et al., 1982; Lundström et al., 2000). Although theories involving eluvial and illuvial organic compounds and aluminosilicates through adsorption, precipitation, and microbial degradation are partly contradictory (e.g., Malcolm and McCracken, 1968; Farmer et al., 1980; Anderson et al., 1982; Buurman and van Reeuwijk, 1984; Little, 1986; Lundström et al., 2000), some processes can act simultaneously. Biogeochemical interactions are consensual, as well as the formation of organic compounds, with a key role in the genesis of the spodic horizon (Lundström et al., 2000).

Amazon Podzols (Spodosols) have been traditionally described in classical studies, which revealed their chemical, mineralogical, and micromorphological attributes, and the possible genesis (Klinge, 1965; Sombroek, 1966; Lucas et al., 1984; Bravard and Righi, 1990; Dubroeuq et al., 1991; Andrade et al., 1997; McClain et al., 1997; Mafra et al., 2002; Patel-Sorrentin et al., 2007; Mendonça et al., 2014). Also, studies in French Guiana and Brazil have shown that Podzols can be formed from various parent materials by the transformation of an initial clayey Oxisol cover (Lucas et al., 1984; Dubroeuq et al., 1991; Andrade et al., 1997); in which Podzols are considered a final degradation stage of the tropical soil cover under a dominant humid equatorial climate (Boulet et al., 1984; Mafra et al., 2002). Other studies indicate a sequence of soil development ranging from Podzol to Histosols, with thick peat layers in the bottom valleys (Dubroeuq and Volkoff, 1998; Bonifacio et al., 2006), often affected by frequent flooding.

While most Podzols studied in Amazonia are close to the rivers and under hydromorphic conditions of the bottomlands, the Serra do Divisor sandy soils are found on elevations and steep slopes, representing very contrasting pedo-environments to date, the only previous study of soils from the Serra do Divisor and Moa river floodplain is the RADAMBRASIL Project (Carvalho et al., 1977). For most Amazon floodplain soils, some characteristics are well known, like the richer-nutrient sediments afforded by the Andean/sub-Andean influence and source, which renew the chemical status by annual floods (Sombroek, 2000; Schaefer et al., 2017). Nevertheless, in the Acre basin (Upper Amazon) influence the extent of sub-Andean has not been investigated, and soil formation remains poorly studied (Schaefer et al., 2017).

In the present study, we examine representative in situ soils of Serra do Divisor, as well as Alluvial (allochthonous) soils of the Moa river floodplain, to enhance the

knowledge on the genesis of these low mountain Podzols and floodplain soil of the Moa river basin.

MATERIALS AND METHODS

Study area

The study area is located in the northwestern part of the Acre State (Brazil), between 73° 40' 20" W / 7° 26' 20" S and 73° 39' 10" W / 7° 27' 18" S (Figure 1). It is part of the National Park of Serra do Divisor, at the westernmost part of Brazil, near the border with Peru. Koppen's Af climates predominate (tropical), without well defined dry seasons (Alvares et al., 2013), under a typical udic moisture regime. The annual mean temperature is 25.5 °C; July is the coldest month with mean temperatures of 24.1 °C, and the warmest month is January with 26.0 °C (Climate-Data.org, 2020). The mean annual rainfall ranges from 2,500 to 2,750 mm (IBGE, 1994).

The geology of Serra do Divisor is composed of distinct stratigraphic units, with a basement of metamorphic and igneous Pre-cambrian to Paleozoic rocks of limited outcrops. Overlying, folded Cretaceous sandstones (Km: Moa formation; Kra: Rio Azul formation; Kd: Divisor formation) are widespread (Carvalho et al., 1977) and represent the parental materials of all soils studied. These sedimentary rocks (Km, Kra, Kd) are composed mostly of quartz-rich sediments, forming in situ, colluvial deposits, and unconsolidated sediments (Qai) (Carvalho et al., 1977; IBGE, 1994). The tectonic evolution of this area indicates a Cretaceous basin open to the Pacific, where mature sandy sediments eroded from the Brazilian continental landmass were deposited (Rossetti et al., 2005). The Andean elevation started in the mid-tertiary and drastically changed the landscape, causing the inversion of the sedimentary basin and drainage network, from the original pacific outlet to the present-day Atlantic, in the Late Cenozoic (Plio-Pleistocene) (Carvalho et al., 1977).

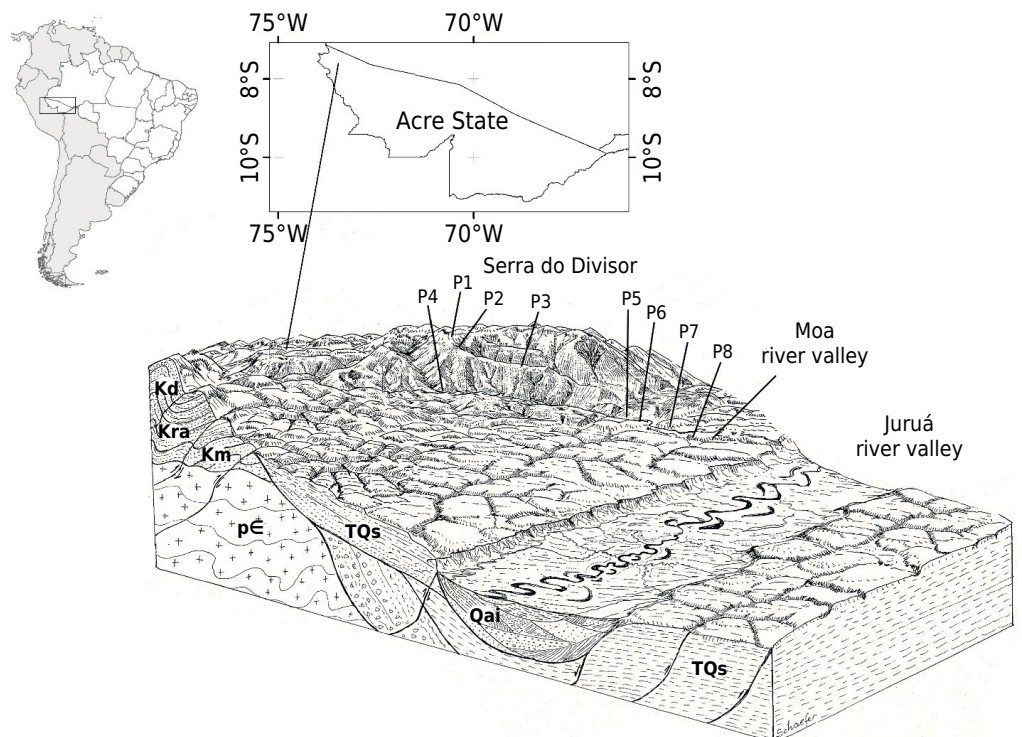


Figure 1. Relative landscape position of the studied soils in the Serra do Divisor and Moa river valley, northwestern of Acre, and location of the Acre State in South America. Geologic substrate symbols: TQs is the Solimoes formation; Qai are Holocene alluvial sediments; Km is the Moa formation; Kra is the Rio Azul formation; Kd is the Divisor formation; pE are the Pre-Cambrian to Paleozoic sediments rocks [Source: adapted from Schaefer et al. (2013)].

At the foot slopes of the Serra do Divisor mountains, Cenozoic sediments are widespread, forming in a regional scale a gentle, dissected relief, at about 200 m a.s.l., formed by Plio-Pleistocene deposits (Solimões formation - TQs) and Holocene alluvial sediments (Qai) of the Moa and Juruá river (Figure 1). Locally, the Solimões formation encompasses mostly argillites and siltites of continental origin, deposited in a floodplain-lacustrine-swampy environment with local gypsum veins and calcareous concretions are present (Carvalho et al., 1977; Latrubesse et al., 2010). The Moa river crosses the Serra do Divisor mountain through a series of faulted lines, forming a canyon, reaching the Juruá floodplain across the dissected lowlands (Figure 1).

Overall, the northwestern part of Acre is covered by typical lowland Tropical Forest, characterized by the Open and Dense physiognomies. It is one of the richest floristic regions worldwide in terms of palm species (Silveira and Daly, 1997). However, in the Serra do Divisor, a type of Submontane Dense Forest is present where unusual highland species occur (Carvalho et al., 1977). In addition, a typical vegetation of the eastern low Andean elevation, regionally named Ceja Forest, is also present, which is characterized by small trees, ferns, shrubs, orchids, mosses, epiphytes and, notably, by abundant Bromeliaceae (Lathrap, 1970).

Soil sampling

Eight representative soils of two main landforms of the Serra do Divisor National Park were studied (Table 1). We selected and sampled an altitudinal sequence at the Serra do Divisor composed of four soils that represent different geomorphic settings and vegetation types: P1 - Typic Haplorthods (*Espodosolo Ferrihumilúvico Órtico arênico*), P2 - Spodic Quartzipsamment (*Neossolos Quartzarênicos Órticos espódicos*), P3 - Lithic Quartzipsamment (*Neossolo Litólico Hístico típico*), and P4 - Lithic Quartzipsamment (*Neossolo Litólico Distrófico fragmentário*). Along the Moa river floodplain, four soils were studied: P5 - Typic Udifluent (*Neossolo Flúvico Distrófico típico*), P6 - Typic Kandiuult (*Argissolo Vermelho-Amarelo Alítico típico*), P7 - Typic Kandiuult (*Argissolo Amarelo Eutrófico abruptico*), and P8 - Arenic Plinthic Kandiuult (*Plintossolo Argilúvico Distrófico arênico*).

Soil pits were dug manually, followed by a morphological description (Santos et al., 2005). Samples of genetic horizons and important horizon boundaries (undisturbed) were collected and submitted to chemical, physical, mineralogical, and micromorphological analysis. The soils were classified according to the Soil Taxonomy (Soil Survey Staff, 2014a) and Brazilian Soil Classification System (Santos et al., 2018).

Table 1. General characteristics of the studied soils at the Serra do Divisor National Park, State of Acre, Brazil

ID	Soil class	Vegetation type	Geology
<i>Serra do Divisor topossequence</i>			
P1	Typic Haplorthods/ <i>Espodosolo Ferrihumilúvico Órtico arênico</i>	Ceja Forest	Moa formation
P2	Spodic Quartzipsamment/ <i>Neossolos Quartzarênicos Órticos espódicos</i>	Ceja Forest	Moa formation
P3	Lithic Quartzipsamment/ <i>Neossolo Litólico Hístico típico</i>	Submontane Dense Forest	Moa formation
P4	Lithic Quartzipsamment/ <i>Neossolo Litólico Distrófico fragmentário</i>	Open Forest with Palms	Moa formation
<i>Moa river floodplain</i>			
P5	Typic Udifluent/ <i>Neossolo Flúvico Distrófico típico</i>	Alluvial Open Forest	Holocene Alluvial sediments
P6	Typic Kandiuult/ <i>Argissolo Vermelho-Amarelo Alítico típico</i>	Pasture	Solimões formation
P7	Typic Kandiuult/ <i>Argissolo Amarelo Eutrófico abruptico</i>	Alluvial Open Forest	Solimões formation
P8	Arenic Plinthic Kandiuult/ <i>Plintossolo Argilúvico Distrófico arênico</i>	Alluvial Open Forest	Holocene Alluvial sediments

Analysis

Soil samples were air-dried and passed through a 2 mm sieve, to obtain air-dried fine earth (ADFE). Soil colours (dry and moist) were obtained using the Munsel Colour Chart. Particle size analysis was based on wet sieving, dispersion, and sedimentation, followed by siphoning of the <math><0.002\text{ mm}</math> fraction (Ruiz, 2005).

All routine analytical chemical and physical measurements were obtained using standard procedures (Sparks et al., 1996; Claessen, 1997). The following properties were determined: pH(H₂O) and pH(KCl) in KCl 1 mol L⁻¹ with a soil:solution ratio of 1:2.5; available P, exchangeable Na and K extracted with Mehlich-1 (P was determined spectrophotometrically; Na and K by flame emission photometry); exchangeable Ca and Mg by atomic absorption spectroscopy and exchangeable Al by titration after extraction with KCl 1 mol L⁻¹ and potential acidity (H+Al) by titration after extraction with calcium acetate 0.5 mol L⁻¹ at pH 7.0. We also evaluated P adsorption by soils through measuring the P remaining (Prem) in a CaCl₂ 10 mmol L⁻¹ solution, with P 60 mg L⁻¹, is put in shaken with a soil sample (Novais and Smyth, 1999; Alvarez et al., 2000; Donagemma et al., 2008). The total organic carbon (TOC) of ADFE was determined by titration of K₂Cr₂O₇ with 0.2 mol L⁻¹ Fe (NH₄)₂(SO₄)₂·6H₂O after wet oxidation treatment (Yeomans and Bremner, 1988).

The mineralogy of clay fraction was determined for all horizons with X-ray diffraction (XRD) analysis, using monochromated CuK α radiation on oriented samples. Were selected samples of the diagnostic horizons to identify the 2:1 clay minerals. The selected samples were saturated with potassium (KCl 1 mol L⁻¹) and magnesium (MgCl₂ 1 mol L⁻¹), submitted to heating (350 °C for the samples saturated with K⁺) and treated with glycerol 10 % (for Mg-saturated samples). The diffractograms were interpreted according to Chen (1977). Amorphous Fe and Al were extracted with ammonium oxalate (McKeague and Day, 1966) and the free iron oxides with dithionite-citrate-bicarbonate (Mehra and Jackson, 1960). To extract the organic bounds forms, we used pH 10.0 sodium pyrophosphate (Soil Survey Staff, 2014b). Iron, Al, and Si were determined by atomic absorption spectrometry.

Soil humic substances were chemically fractionated by the alkali and acid solubility, according to Swift (1996), adapted by Mendonça and Matos (2005).

The micromorphology of the diagnostic horizons of P1, P2, P5, and P6 was investigated in thin sections (Table 2), following the recommendations of Stoops et al. (2018), using a petrographic microscope Olympus CH30. Semi-Quantitative elementary analysis and microchemical maps were obtained after stoichiometric normalization by ZAF procedures using electron microscopy and EDS analyses (LEO Zeis - 430i model operated in 84 eV).

RESULTS

Soils of Serra do Divisor

All soils studied at *Serra do Divisor* are sandy with high amounts of coarse and fine sand and less than 10 % of clay and 11 % of silt (Table 3), being derived from Cretaceous weathered sandstone. They are nutrient-poor, extremely dystrophic, with very low cation exchange capacity (CEC), high Al saturation and high amounts of total organic carbon (TOC) (Table 3). All soils have an expressive accumulation of organic material in the surface horizons, reaching 306.6 g kg⁻¹ in the O horizon of P3 (Table 4). Nutrient contents decrease with depth in all soils, along with reduced TOC levels and increase in pH (Table 4).

The physical properties of soils from *Serra do Divisor*, with a sandy texture, associated with high rainfall, favor the migration of organic compounds, as confirmed by the

Table 2. Thin sections of the diagnostic horizon of P1, P2, P5, P6, P7, and P8 investigated on the electronic microscope and submitted to qualitative EDS analyses

Profile	Horizon	Layer	Macromorphological structure
		m	
P1 - Typic Haplorthods/ <i>Espodosolo Ferrihumilúvico Órtico arênico</i>	Bhs	0.35-0.70	Weak coarse subangular blocky structure
P2 - Spodic Quartzipsamments/ <i>Neossolos Quartzarênicos Órticos espódicos</i>	C2	0.70-0.90	Single grain
P5 - Typic Udifluvents/ <i>Neossolo Flúvico Distrófico típico</i>	C1	0.08-0.20	Single grain
P5 - Typic Udifluvents/ <i>Neossolo Flúvico Distrófico típico</i>	2C4	1.00-1.10	Strong coarse prismatic structure
P6 - Typic Kandiudults/ <i>Argissolo Vermelho-Amarelo Alítico típico</i>	Bt1	0.13-0.30	Strong medium and coarse subangular blocky
P6 - Typic Kandiudults/ <i>Argissolo Vermelho-Amarelo Alítico típico</i>	Bt2	0.30-0.55	Strong medium subangular blocky
P6 - Typic Kandiudults/ <i>Argissolo Vermelho-Amarelo Alítico típico</i>	Bt3	0.55-1.00	Strong medium and coarse subangular blocky
P7 - Typic Kandiudalts/ <i>Argissolo Amarelo Eutrófico abruptico</i>	Bt	0.15-0.40	Moderate to strong medium and coarse subangular blocky
P8 - Arenic Plinthic Kandiudult/ <i>Plintossolo Argilúvico Distrófico arênico</i>	Btv1	0.85-1.10	Strong small and medium subangular blocky

subsurface TOC data (Table 3), forming Al-rich organic coating on quartz grains (Figure 2). In the Spodosol (P1) and Entisol (P2), TOC values increase from 0.35 to 0.70 m depths and from 0.70 to 0.90 m depths, respectively, indicating active podzolization (Table 4). For P1, macromorphological features showed a subangular blocky structure for the Bhs horizon (Table 2).

All soils showed kaolinite mineralogy (major reflections at 7.22 Å and 3.58 Å), with traces of quartz and gibbsite (Table 5 and Figure 3).

For P1, the high amounts of Al extracted by ammonium oxalate and sodium pyrophosphate and the high Fe_o/Fe_d ratio (Table 5) in the Bhs are associated with high TOC, which indicate the accumulation of poorly crystalline illuvial organometallic complexes formed in the spodic horizon (Figure 2). In P1, the Bs and Bhs horizons had the highest value of Fe_o/Fe_d ratio, nearing 1.0 (Table 5), suggesting the presence of ferrihydrite (Schwertmann et al., 1986). Another poorly crystalline mineral occurring in this soil is imogolite, indicated by the $Al_o - Al_p$ difference or/and the $Al_o + \frac{1}{2} Fe_o > 0.5$ ratio (Ugolini and Dahlgren, 1991; Soil Survey Staff, 2014a,b).

In the C2 horizon of P2, the accumulation of illuvial organometallic complexes is similar to Bs horizon of P1, but insufficient to define a spodic horizon, due to low Al_o , Fe_o , and TOC values. The point-source microanalysis of C2 horizon in P2 and the chemistry and mineralogy properties reveal a predominantly kaolinitic composition of the micromass with Fe oxide and fine coatings of organic matter with Al phases on subangular to subrounded quartz grains (Figure 4). The K amounts in the groundmass are much lower than in the inner feldspar crystals, due to the high mobility and lixiviation of this cation (Figure 4). In this layer, we also verified the presence of gibbsite by XRD (Figure 3), suggesting deep weathering.

The P3 and P4 present similar values to P2 of Al and Fe extracted by oxalate and DCB. However, P4 has higher levels of Fe_d indicating more crystalline Fe phases and the

Table 3. Physical properties of the <2 mm fraction of the studied soils

Horizon	Layer	Munsell color		Sand ⁽¹⁾		Silt ⁽¹⁾	Clay ⁽¹⁾
		Dry	Moist	Coarse	Fine		
	m	g kg ⁻¹					
P1 - Typic Haplorthods (<i>Espodosolo Ferrihumilúvico Órtico arênico</i>)							
O	0.40-0.00	7.5YR 2.5/3	7.5YR 2/2	-	-	-	-
A	0.00-0.10	10YR 5/2	10YR 2/1	570	320	70	40
E	0.10-0.35	10YR 6/3	10YR 4/3	550	380	50	20
Bs	0.35-0.45	10YR 3/2	10YR 5/4	600	330	30	40
Bhs	0.35-0.70	10YR 4/4	10YR 2/1	550	310	50	90
CR	0.70-0.80 ⁺	10YR 5/3	10YR 3/3	490	460	10	40
P2 - Spodic Quartzipsamments (<i>Neossolos Quartzarênicos Órticos espódicos</i>)							
O	0.50-0.00	7.5YR 2.5/3	7.5YR 2/2	-	-	-	-
A	0.00-0.15	10YR 4/3	10YR 2/2	610	290	20	80
C1	0.15-0.70	10YR 5/3	10YR 2.5/2	720	240	30	10
C2	0.70-0.90	10YR 4/4	10YR 2/2	810	120	30	40
CR	0.90 ⁺	-	-	-	-	-	-
P3 - Lithic Quartzipsamments (<i>Neossolo Litólico Hístico típico</i>)							
O	0.30-0.00	7.5YR 3/3	7.5YR 2.5/3	-	-	-	-
A	0.00-0.10	10YR 4/3	10YR 2/2	710	150	40	100
C	0.10-0.40	10YR 6/4	10YR 3/4	690	190	20	100
P4 - Lithic Quartzipsamments (<i>Neossolo Litólico Distrófico fragmentário</i>)							
O	0.10-0.00	10YR 5/3	10YR 3/3	-	-	-	-
A	0.00-0.50	10YR 5/4	10YR 3/4	550	320	60	70
AC	0.50-0.15	10YR 5/6	10YR 4/4	520	310	110	60
C	0.15-0.35	10YR 7/6	10YR 4/6	620	260	70	50
CR	0.35-0.50 ⁺	10YR 6/8	7.5YR 5/8	-	-	-	-
P5 - Typic Udifluvents (<i>Neossolo Flúvico Distrófico típico</i>)							
A	0.00-0.80	10YR 6/3	10YR 4/3	0	820	110	70
C1	0.80-0.20	10YR 7/4	10YR 5/4	20	840	80	60
C2	0.20-0.30	10YR 8/4	10YR 6/4	20	920	30	30
C3	0.30-1.00	10YR 8/2	10YR 7/4	70	890	20	20
2C4	1.00-1.10	5YR 6/8	5YR 5/8	150	240	370	240
P6 - Typic Kandiuults (<i>Argissolo Vermelho-Amarelo Alítico típico</i>)							
A	0.00-0.10	10YR 6/2	7.5YR 4/2	100	330	330	240
AE	0.10-0.13	10YR 6/3	7.5YR 6/3	90	370	320	220
Bt1	0.13-0.30	7.5YR 6/6	7.5YR 4/4	70	260	290	380
Bt2	0.30-0.55	7.5YR 7/6 5YR 6/6	7.5YR 6/6 5YR 5/6	60	200	280	460
Bt3	0.55-1.00	5YR 5/6 10YR 7/6	5YR 5/8 2.5Y 6/6	60	200	280	460
C	1.00-1.20	2.5YR 6/8	2.5YR 5/8	30	140	320	510
P7 - Typic Kandiuults (<i>Argissolo Amarelo Eutrófico abrutico</i>)							
A	0.00-0.15	10YR 6/3	10YR 4/3	30	770	130	70
Bt	0.15-0.40	10YR 7/3	10YR 4/4	0	60	620	320
BC	0.40-0.70	10YR 6/8 10YR 8/2	7.5YR 5/6 10YR 7/1	0	10	470	520

continue...

continuation

		7.5YR 6/8	7.5YR 5/8				
C	0.70-1.20	2.5Y 7/1	7.5YR 5/1	10	10	380	600
		10YR 8/3	7.5YR 6/3				
<i>P8 – Arenic Plinthic Kandiodults (Plintossolo Argilúvico Distrófico arênico)</i>							
A	0.00-0.10	10YR 6/2	10YR 3/2	10	840	90	60
E1	0.10-0.20	10YR 7/2	10YR 5/3	10	910	30	50
2E2	0.20-0.30	10YR 6/2	10YR 4/2	0	810	120	70
3E3	0.30-0.50	10YR 8/3	10YR 6/4	0	730	180	90
4E4	0.50-0.85	10YR 8/2	10YR 5/4	10	930	10	50
		7.5YR 5/8	7.5YR 4/6				
Btv1	0.85-1.10	10YR 8/1.5	10YR 7/1.5	0	20	360	620
		5YR 5/6	5YR 3/4				
Bt2	1.10-1.30	10YR 8/1	10YR 6/2	30	290	300	380
		10YR 3/1	10YR 3/0.5				
C	1.30-1.50	10YR 8/2	10YR 7/1.5	10	680	120	190
		7.5YR 6/8	7.5YR 5/8				

⁽¹⁾ Particle size according to the method described by Ruiz (2005).

presence of Al-goethite by XRD, also suggested by the yellowish color. The Al-goethite was indicated by the dithionite-citrate-bicarbonate extraction (Al_d and Fe_d , Table 5), and also by a peak shift to higher angles in XRD of the goethite (Schwertmann and Cornell, 2000).

Regarding the humic fractions, there is a small increase the fulvic acids fraction (FA) in the subsurface horizons of P1, P2, and P3 (Table 6). The P1 has accumulation of FA and humic acid fractions (HA) in the Bhs horizon (Table 6).

The P1 and P2 showed clear podzolized horizons (Bhs and C2, respectively) with many illuvial features, like organic coatings (or organs) (Figure 2 and Table 7) (Brewer, 1973; Paton, 1978). The backscattered electrons images of P1 (Bhs horizon) and P2 (C2 horizon) (Figure 2) revealed the macroporosity with the prevalence of subangular/subrounded quartz grains, which favor the downward migration of the organic metal complexes in the soils. The Bhs horizon of P1 has a greater relative micromass proportion, which is related to its well-developed macrostructure. These pedo-environments present local bridged-grain microstructure, biologic channels, organic compound coatings, nodules, pellety, and partially decomposed organic fragments (Table 7), with clear evidence of bioturbation. Ferruginous concretions also occur but in low amounts, due to the coarse texture and the low content of ferruginous material in the sandstone substrate (Table 7). In the C2 horizon of P2, we found OM illuvial features (Figure 4 and Table 7), associated with Al forms and, in a lesser amount, Fe forms; and fine K-feldspar grains.

Moa river floodplain soils

The soils of the Moa river floodplain are considerably richer in nutrients than soils on sandstones of Serra do Divisor. Enhanced microbial activity results in organic matter mineralization, as indicated by the low levels of organic carbon and the small amounts of OM at the topsoil for all soils (Table 3).

Except for P5, which is closer to the Serra do Divisor (Figure 1) and local influence of the Moa formation, all other floodplain soils occur on the Solimões Formation or on the

Table 4. Chemical characteristics of the <2 mm fraction of the studied soils

Horizon	Layer m	pH(H ₂ O)	P ⁽¹⁾	K ⁺⁽¹⁾	Na ⁺⁽¹⁾	Ca ²⁺⁽²⁾	Mg ²⁺⁽²⁾	Al ³⁺⁽³⁾	H + Al ⁽⁴⁾	CEC ⁽⁵⁾	BS ⁽⁶⁾	Prem ⁽⁷⁾	m ⁽⁸⁾	TOC ⁽⁹⁾
			mg dm ⁻³				cmol _c kg ⁻¹				%	mg L ⁻¹	%	g kg ⁻¹
P1 – Typic Haplorthods (<i>Espodosolo Ferrihumilúvico Órtico arênico</i>)														
O	0.40-0.00	3.38	16	0.22	0.04	0	0.04	2.36	39.1	39.4	0.8	58.3	89	293.6
A	0.00-0.10	3.65	5.3	0.07	0	0	0.03	1.06	13.5	13.6	0.7	54.1	91	29.5
E	0.10-0.35	4.21	1.5	0.02	0	0	0.01	0.43	3.2	3.23	0.9	50.9	93	4.2
Bs	0.35-0.45	4.47	0.9	0.01	0	0.03	0.03	0.72	8.6	8.67	0.8	26.7	91	8.0
Bhs	0.35-0.70	4.66	1.4	0.01	0	0	0.02	1.06	19.7	19.7	0.2	6.8	97	29.3
CR	0.70-0.80 ⁺	5.18	1.3	0.01	0	0	0.01	0.19	4.1	4.12	0.5	25.2	90	5.3
P2 – Spodic Quartzipsamments (<i>Neossolos Quartzarênicos Órticos espódicos</i>)														
O	0.50-0.00	3.67	15	0.56	0.01	0	0.08	2.07	31.2	31.8	2.0	57.5	76	253.4
A	0.00-0.15	4.20	4.1	0.15	0	0	0.05	1.16	13.4	13.6	1.5	34	85	2.5
C1	0.15-0.70	4.63	0.9	0.02	0	0	0.01	0.39	4.9	4.93	0.6	34.8	93	5.2
C2	0.70-0.90	5.01	2.1	0.02	0	0	0.02	0.43	8.1	8.14	0.5	16.5	92	7.0
P3 – Lithic Quartzipsamments (<i>Neossolo Litólico Hístico típico</i>)														
O	0.30-0.00	3.91	16	0.48	0.01	0	0.08	1.35	17	17.6	3.2	56.2	70	306.6
A	0.00-0.10	3.76	6.0	0.14	0	0	0.05	1.16	13.7	13.9	1.4	45.4	86	34.9
C	0.10-0.40	4.26	1.4	0.06	0	0	0.02	0.92	8.1	8.18	1	23.1	92	10.5
P4 – Lithic Quartzipsamments (<i>Neossolo Litólico Distrófico fragmentário</i>)														
O	0.10-0.00	4.67	16	0.34	0	1	0.21	0.72	8.6	10.2	15.3	43.3	32	47.9
A	0.00-0.50	5.02	3.2	0.07	0	0	0.05	0.43	6.8	6.92	1.7	27.5	78	15.8
AC	0.50-0.15	5.55	3.3	0.05	0	0.01	0.04	0.29	5.7	5.8	1.7	22.1	74	18.7
C	0.15-0.35	5.23	1.4	0.02	0	0	0.02	0.19	3.5	3.54	1.1	27.4	83	20.9
P5 – Typic Udifluvents (<i>Neossolo Flúvico Distrófico típico</i>)														
A	0.00-0.80	5.09	7.1	0.18	0	2.86	0.73	0.05	4	7.77	48.5	47.1	1	17.7
C1	0.80-0.20	4.92	3.4	0.14	0	1.16	0.28	0.43	1.9	3.48	45.4	36.9	21	2.0
C2	0.20-0.30	5.18	1.6	0.06	0	0.75	0.27	0.43	1.4	2.48	43.5	40.4	28	2.3
C3	0.30-1.00	5.40	3.4	0.04	0	0.48	0.14	0.39	1.1	1.76	37.5	47.4	37	0.5
2C4	1.00-1.10	4.98	1.6	0.12	0.01	5.04	0.69	2.26	8.1	14	42.0	15.4	28	5.2
3C5	1.10-1.40	5.45	4.0	0.05	0	1.90	0.31	0.34	1.9	4.16	54.3	40.8	13	1.4
P6 – Typic Kandiuults (<i>Argissolo Vermelho-Amarelo Alítico típico</i>)														
A	0.00-0.10	4.95	9.1	0.27	0.05	2.84	0.79	0.67	8.1	12.1	32.8	20.5	14	24.1
AE	0.10-0.13	5.01	3.5	0.14	0.05	2.91	0.58	0.96	7.3	11	33.5	17.1	21	16.7
Bt1	0.13-0.30	4.95	1.3	0.13	0.04	1.63	0.27	3.66	12.4	14.5	14.3	2.7	64	8.2
Bt2	0.30-0.55	4.91	1.1	0.14	0.02	0.79	0.11	4.77	16.2	17.3	6.1	3.1	82	5.5
Bt3	0.55-1.00	4.91	2.0	0.10	0	0.12	0.04	4.77	16.2	16.5	1.6	1.3	95	3.8
C	1.00-1.20	5.01	0.8	0.13	0	0.02	0.04	3.81	14.2	14.4	1.3	3.5	95	2.9
P7 – Typic Kandiualfs (<i>Argissolo Amarelo Eutrófico abruptico</i>)														
A	0.00-0.15	5.18	3.9	0.26	0	2.70	0.92	0.05	3.3	7.18	54	45	1	11.4
Bt	0.15-0.40	4.88	1.9	0.16	0.01	9.57	1.86	2.36	9.4	21	55.2	12	17	9.9
BC	0.40-0.70	4.98	1.6	0.20	0.04	9.50	1.99	4.29	14.5	26.2	44.7	6.3	27	5.8
C	0.70-1.20	5.05	2.2	0.25	0.05	10.90	2.20	4.87	17	30.4	44	4.6	27	3.8
P8 – Arenic Plinthic Kandiuults (<i>Plintossolo Argilúvico Distrófico arênico</i>)														
A	0.00-0.10	5.06	3.3	0.16	0	1.94	0.48	0.05	3.0	5.58	46.2	47.9	2	8.8
E1	0.10-0.20	4.93	2.2	0.06	0	1.22	0.22	0.19	2.2	3.70	40.5	46.4	11	6.4
2E2	0.20-0.30	4.88	2.0	0.07	0	1.55	0.20	0.39	3.2	5.02	36.3	39.9	18	7.6
3E3	0.30-0.50	5.3	1.5	0.06	0	1.67	0.42	0.43	2.5	4.65	46.2	35.6	17	3.7
4E4	0.50-0.85	5.43	3.1	0.03	0	0.73	0.17	0.43	1.4	2.33	39.9	40.2	32	0.3
Btv1	0.85-1.10	5.13	2.3	0.25	0.08	10.20	3.16	4.19	14.2	27.90	49.1	4	23	9.9
Bt2	1.10-1.30	5.01	1.5	0.14	0.03	1.25	0.51	3.90	13.4	15.30	12.6	6.5	67	5.8
C	1.30-1.50	4.89	3.4	0.08	0	0.18	0.12	1.98	7.2	7.58	5	12	84	2.0

⁽¹⁾ Extracted with Mehlich-1 (P was determined spectrophotometrically; and Na and K by flame emission photometry). ⁽²⁾ Extracted with KCl 1 mol L⁻¹ and determined by atomic absorption spectroscopy. ⁽³⁾ Determined by titration after extraction with KCl 1 mol L⁻¹. ⁽⁴⁾ Determined by titration after extraction with calcium acetate 0.5 mol L⁻¹ at pH 7.0. ⁽⁵⁾ CEC: cation exchange capacity; ⁽⁶⁾ BS: base saturation; ⁽⁷⁾ Prem: P remaining in a CaCl₂ 10 mmol L⁻¹ solution, with P 60 mg L⁻¹ (Novais and Smyth, 1999; Alvarez et al., 2000; Donagemma et al., 2008); ⁽⁸⁾ m = [Al³⁺/(Na⁺ + K⁺ + Ca²⁺ + Mg²⁺ + Al³⁺)] × 100; ⁽⁹⁾ TOC: total organic carbon determined by titration of K₂Cr₂O₇ with Fe (NH₄)₂(SO₄)₂·6H₂O 0.2 mol L⁻¹ after wet oxidation treatment (Yeomans and Bremner, 1988).

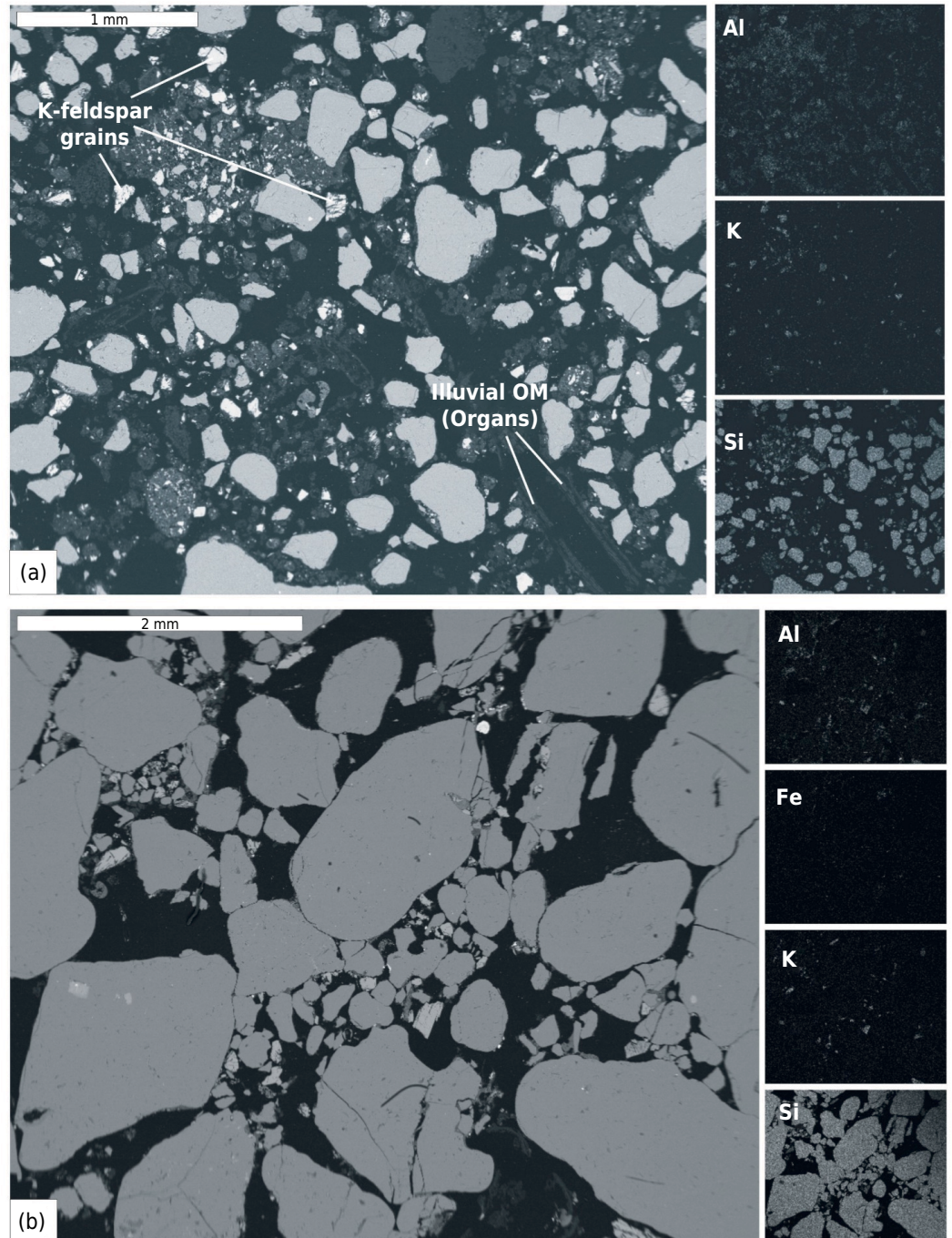


Figure 2. Backscattered electrons images and microchemical maps of pedogenic horizons. (a) P1, Bhs horizon (0.35-0.70 m) with illuvial Al-rich organic matter coating features, and rare K-feldspar grains. (b) P2, C2 horizon (0.70-0.90 m) with Al-rich organic matter, little Fe forms, and rare K-feldspar grains.

Holocene Alluvial sediments (Table 1). A pedological discontinuity from 1.00 to 1.10 m in P5, is indicated by increasing clay content, which results in higher levels of Na, Ca^{2+} , Al^{3+} , H+Al, and TOC, and a decrease in Prem (Tables 3 and 4) and the absence of illuvial features. Also, figure 5 shows differences in c/f (coarse/fine) relation distribution for C1 and 2C4 horizons of P5, enaulic and chitonic, respectively.

The P6 has an increment of clay with depth, higher than 1.7 times the clay content of the overlying eluvial horizon (Table 3), and with some coatings of oriented clay on the surface of peds (Table 7), suggesting argilluviation. The P6 had a base saturation lower than 34 %, decreasing with depth.

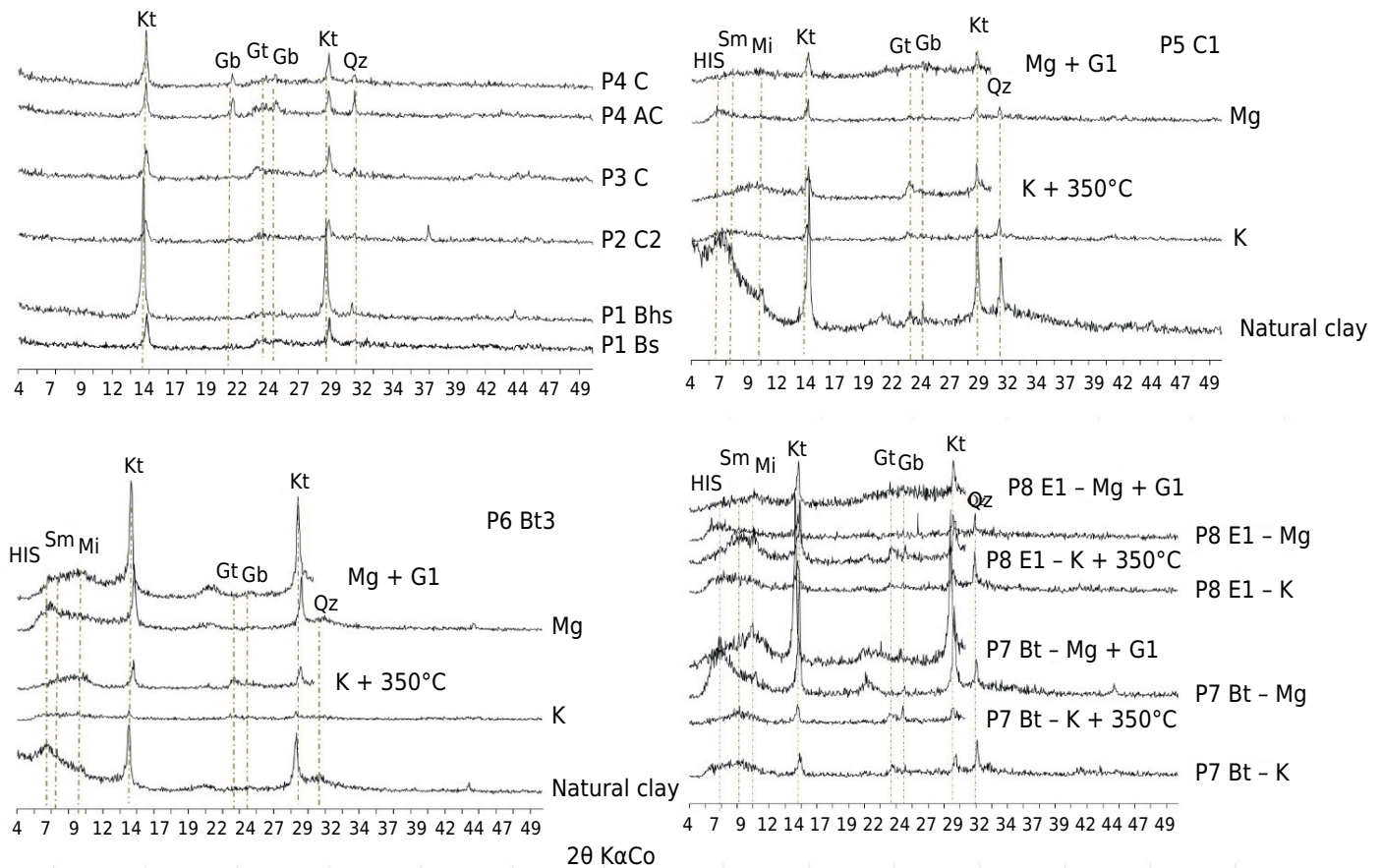


Figure 3. X-ray diffraction of natural clay fractions (P1 to P4) and treated clay samples (P5 to P8). Kt: kaolinite; Gb: gibbsite; Qz: quartz; Gt: goethite; Sm: smectite; Mi: mica; HIS: hydroxyl-Al interlayered smectite.

The P7 is the only eutrophic soil (BS ≥ 50 %), with an argillic horizon and abrupt textural change. The argillic horizon has a four-fold increment of clay content in relation to the overlying horizon (Table 3). The loamy and silty substrates of Solimões formation favor well developed aggregates (peds), as present in P6 and P7, and a subangular blocky structure (Table 2).

In P8, the sedimentary discontinuity in the subsurface, indicated by abrupt differences in particle size, distinct color layers, and the absence of illuvial features, are important properties, which are related to changing fluvial deposition. At the Btv1 horizon, there is an abrupt increase in clay accompanied by a slight increase in organic C (Tables 3 and 4). This is related to a sandy material overlaying clayey sediment, with higher organic C content, typical of meandering rivers. Plinthite occurrence was confirmed by laboratory test, which shown iron concretions remained firm when moist and became irreversibly hardened after exposed to the atmosphere and repeated wetting and drying (Soil Survey Staff, 2014a), and confirmed by pedogenic analyses (Table 7). Micromorphology indicates an incipient pedological development and association with hydromorphic features, like massive reducing (bleached) zones, intense polychromy, rare biological channels, absence of illuvial features, depletion zones by ferrolysis and gleization, and also a collapsing structure with the destruction of clay and clogging of pores with dispersed material (Table 7). All these features point a prolonged hydromorphism.

At Moa river alluvial soils (P5 to P8), we identified mixed mineralogy, with coexisting gibbsite (4.86 Å), kaolinite (major reflections at 7.22 and 3.58 Å), smectite and/or vermiculite (14.2-17.1 Å for Mg and glycerol saturated samples) (Figure 3), representing mixed sources of a sedimentary load.

Table 5. Clay mineralogy by DRX, Al_d, Al_o, Al_p, Fe_d, Fe_o, Fe_p, Si_p, and some ratios of the studied soils

Horizon	Layer	Al _d ⁽¹⁾	Al _o ⁽²⁾	Fe _d ⁽¹⁾	Fe _o ⁽²⁾	Al _p ⁽³⁾	Fe _p ⁽³⁾	Si _p ⁽³⁾	Fe _o /Fe _d	Al _o -Al _p	Al _o -1/2Fe _o	Clay mineralogy ⁽⁴⁾
	m	%										
P1 – Typic Haplorthods (<i>Espodossolo Ferrihumilúvico Órtico arênico</i>)												
A	0.00-0.10	0.11	0.07	0.04	0.01	0.33	0.05	0.72	0.21	-0.26	0.065	
E	0.10-0.35	0.06	0.03	0	0	0.31	0.04	0.66	0	-0.28	0.030	Kt
Bs	0.35-0.45	0.21	0.19	0.13	0.13	1.49	0.62	1.05	0.98	-1.30	0.125	Kt
Bhs	0.35-0.70	1.24	1.23	0.20	0.20	8.27	1.15	1.54	0.98	-7.04	1.130	Kt>>Gb>Qz
P2 – Spodic Quartzipsamments (<i>Neossolos Quartzarênicos Órticos espódicos</i>)												
A	0.00-0.15	0.21	0.13	0.22	0.10	1.40	0.61	1.04	0.48	-1.27	0.08	
C1	0.15-0.70	0.11	0.10	0.14	0.06	1.08	0.50	0.61	0.42	-0.98	0.07	Kt>>Gb
C2	0.70-0.90	0.33	0.29	0.21	0.08	1.49	0.35	0.52	0.39	-1.20	0.25	Kt>>Gb>Qz
P3 – Lithic Quartzipsamments (<i>Neossolo Litólico Hístico típico</i>)												
A	0.00-0.10	0.16	0.11	0.14	0.04	1.84	0.40	2.26	0.26	-1.73	0.09	
C	0.10-0.40	0.24	0.21	0.25	0.14	3.65	1.06	3.07	0.56	-3.44	0.14	Kt>>Gb>Qz
P4 – Lithic Quartzipsamments (<i>Neossolo Litólico Distrófico fragmentário</i>)												
A	0.00-0.50	0.34	0.23	0.95	0.15	2.00	1.19	0.96	0.16	-1.77	0.155	
AC	0.50-0.15	0.37	0.24	1.09	0.19	3.00	1.94	1.54	0.17	-2.76	0.145	Kt>Gb>Qz>Gt
C	0.15-0.35	0.29	0.18	1.11	0.20	2.16	1.64	1.08	0.18	-1.98	0.080	Kt>Gb>Qz>Gt
P5 – Typic Udifluvents (<i>Neossolo Flúvico Distrófico típico</i>)												
A	0.00-0.80	0.10	0.06	0.27	0.15	-	-	-	0.57	-	-0.015	
C1	0.80-0.20	0.09	0.05	0.25	0.13	-	-	-	0.53	-	-0.015	Kt>Qz>Gb>Sm>Mi>HIS
C2	0.20-0.30	0.07	0.04	0.16	0.11	-	-	-	0.72	-	-0.015	
C3	0.30-1.00	0.05	0.02	0.09	0.07	-	-	-	0.77	-	-0.015	Kt>Qz>Gb>Sm>Mi> HIS
2C4	1.00-1.10	0.24	0.18	1.07	0.64	-	-	-	0.60	-	-0.140	
3C5	1.10-1.40	0.07	0.04	0.26	0.14	-	-	-	0.55	-	-0.030	
P6 – Typic Kandiuults (<i>Argissolo Vermelho-Amarelo Alítico típico</i>)												
A	0.00-0.10	0.33	0.22	1.24	0.89	-	-	-	0.72	-	-0.225	
AE	0.10-0.13	0.37	0.22	1.40	0.79	-	-	-	0.56	-	-0.175	
Bt1	0.13-0.30	0.68	0.34	2.37	0.45	-	-	-	0.19	-	0.115	Kt>Qz>Gt>Gb>Sm>Mi> HIS
Bt2	0.30-0.55	0.87	0.45	2.99	0.40	-	-	-	0.13	-	0.250	
Bt3	0.55-1.00	0.86	0.42	3.05	0.30	-	-	-	0.10	-	0.270	Kt>Qz>Gt>Gb>Sm>Mi> HIS
C	1.00-1.20	0.73	0.41	3.11	0.23	-	-	-	0.07	-	0.295	
P7 – Typic Kandiuults (<i>Argissolo Amarelo Eutrófico abruptico</i>)												
A	0.00-0.15	0.08	0.05	0.27	0.21	-	-	-	0.76	-	-0.055	
Bt	0.15-0.40	0.35	0.26	1.52	0.83	-	-	-	0.54	-	-0.155	Kt>Qz>Gt>Gb>Sm>Mi> HIS
BC	0.40-0.70	0.49	0.40	2.08	0.84	-	-	-	0.41	-	-0.020	
C	0.70-1.20	0.54	0.43	1.96	0.75	-	-	-	0.38	-	0.055	
P8 – Arenic Plinthic Kandiuults (<i>Plintossolo Argilúvico Distrófico arênico</i>)												
A	0.00-0.10	0.06	0.03	0.12	0.11	-	-	-	0.96	-	-0.025	
E1	0.10-0.20	0.05	0.03	0.09	0.10	-	-	-	1.09	-	-0.020	
2E2	0.20-0.30	0.06	0.05	0.14	0.16	-	-	-	1.17	-	-0.030	
3E3	0.30-0.50	0.07	0.07	0.21	0.25	-	-	-	1.23	-	-0.055	
4E4	0.50-0.85	0.05	0.04	0.08	0.10	-	-	-	1.38	-	-0.010	
Btv1	0.85-1.10	0.42	0.45	1.66	1.14	-	-	-	0.69	-	-0.120	Kt>Qz>Gt>Gb>Sm>Mi> HIS
Bt2	1.10-1.30	0.34	0.31	1.47	0.54	-	-	-	0.36	-	0.040	
C	1.30-1.50	0.16	0.17	0.48	0.26	-	-	-	0.54	-	0.040	

⁽¹⁾ Extracted with dithionite-citrate-bicarbonate (Mehra and Jackson, 1960). ⁽²⁾ Extracted with ammonium oxalate (McKeague and Day, 1966). ⁽³⁾ Extracted with sodium pyrophosphate (Soil Survey Staff, 2014b). ⁽⁴⁾ Kt: kaolinite; Gb: gibbsite; Qz: quartz; Gt: goethite; Sm: smectite; Mi: mica; HIS: hydroxyl-Al interlayered smectite.

Table 6. Organic matter fraction and total organic carbon (TOC) of the studied soils

Horizon	Layer	FA ⁽¹⁾	HA ⁽¹⁾	Humin ⁽¹⁾	Total	TOC ⁽²⁾	
	m	g kg ⁻¹					
P1 – Typic Haplorthods (<i>Espodosolo Ferrihumilúvico Órtico arênico</i>)							
O	0.40-0.00					293.6	
A	0.00-0.10	1.5	4.5	16.0	22.0	29.5	
E	0.10-0.35	0.6	1.4	2.0	4.0	4.2	
Bs	0.35-0.45	2.2	2.0	0.8	5.0	8.0	
Bhs	0.35-0.70	8.2	4.9	1.6	14.8	29.3	
CR	0.70-0.80 ⁺	1.0	0.7	1.2	2.9	5.3	
P2 – Spodic Quartzipsamments (<i>Neossolos Quartzarênicos Órticos espódicos</i>)							
O	0.50-0.00					253.4	
A	0.00-0.15	2.5	3.3	15.3	21.1	32.5	
C1	0.15-0.70	0.8	0.8	2.0	3.6	5.2	
C2	0.70-0.90	1.4	0.9	1.6	3.9	7.0	
P3 – Lithic Quartzipsamments (<i>Neossolo Litólico Hístico típico</i>)							
O	0.30-0.00					306.6	
A	0.00-0.10	1.7	3.2	17.6	22.5	34.9	
C	0.10-0.40	2.5	1.6	1.6	5.7	10.5	
P4 – Lithic Quartzipsamments (<i>Neossolo Litólico Distrófico fragmentário</i>)							
O	0.10-0.00					47.9	
A	0.00-0.50	1.8	2.6	3.4	7.8	15.8	
AC	0.50-0.15					18.7	
C	0.15-0.35	1.3	0.4	3.1	4.8	20.9	
P5 – Typic Udifluvents (<i>Neossolo Flúvico Distrófico típico</i>)							
A	0.00-0.80	1.6	3.1	1.6	6.3	17.7	
C1	0.80-0.20	0.7	0.4	1.7	2.8	2.0	
C2	0.20-0.30					2.3	
C3	0.30-1.00					0.5	
2C4	1.00-1.10	0.6	0.2	4.0	4.8	5.2	
3C5	1.10-1.40					1.4	
P6 – Typic Kandiodults (<i>Argissolo Vermelho-Amarelo Alítico típico</i>)							
A	0.00-0.10	1.2	4.3	3.9	9.4	24.1	
AE	0.10-0.13					16.7	
Bt1	0.13-0.30	1.3	2.6	3.7	7.6	8.2	
Bt2	0.30-0.55	1.0	1.9	3.2	6.1	5.5	
Bt3	0.55-1.00					3.8	
C	1.00-1.20					2.9	
P7 – Typic Kandiodalfs (<i>Argissolo Amarelo Eutrófico abruptico</i>)							
A	0.00-0.15	1.1	2.1	1.7	4.9	11.4	
Bt	0.15-0.40	1.6	0.6	6.9	9.2	9.9	
BC	0.40-0.70					5.8	
C	0.70-1.20					3.8	
P8 – Arenic Plinthic Kandiodults (<i>Plintossolo Argilúvico Distrófico arênico</i>)							
A	0.00-0.10	1.1	2.7	2.2	6.0	8.8	
E1	0.10-0.20					6.4	
2E2	0.20-0.30					7.6	
3E3	0.30-0.50	0.8	0.3	2.9	4.0	3.7	
4E4	0.50-0.85					0.3	
Btv1	0.85-1.10	1.3	1.4	6.0	8.7	9.9	
Bt2	1.10-1.30	0.5	1.5	2.4	4.3	5.8	
C	1.30-1.50					2.0	

⁽¹⁾ Fulvic acids fraction (FA), humic acids fraction (HA), and humin, according to methodology described by Swift (1996), adapted by Mendonça and Matos (2005). ⁽²⁾ TOC: total organic carbon according to methodology described by Yeomans and Bremner (1988).

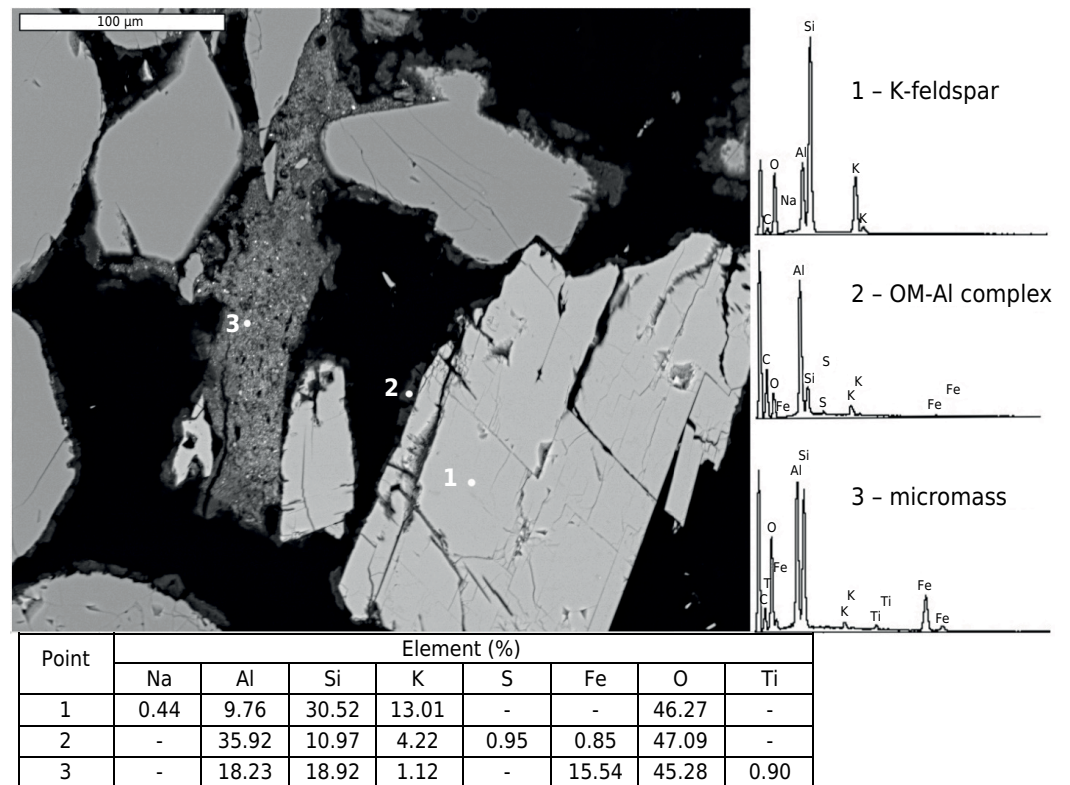


Figure 4. Detailed photomicrographic of C2 horizon of P2 with qualitative and quantitative EDS analyses: (1) K-feldspar crystal; (2) OM-Al complexes with illuvial feature; and (3) micromass.

The diagnostic horizons of P6, P7, and P8 present high Fe_d and low Fe_o/Fe_d ratios suggesting the presence of goethite in the clay fraction, confirmed by the XRD analyses (Table 5). In P8, the Fe_o/Fe_d ratio close to 1.0 in eluvial horizons (2E2, 3E3, and 4E4) can indicate the presence of ferrihydrite. These soils are more yellowish, although the oxidation and reduction process causes mottled zones in subsurface horizons (Table 7) and can be corroborated by the multicolored layers (Table 3).

The alluvial soils of Moa river have a higher variation of TOC values and humic substances with depth, following variable energies of sediment deposition. We did not find any micropedological evidence of carbon illuviation so that an in situ origin for the humic substances is inferred.

The backscattered electrons images of P5 reveal that 2C4 is richer in fine fraction (clay + silt) than C1, due to the sediment discontinuity (Figure 5). In P6 backscattered electrons images of Bt1 horizon, we identified well-developed peds (Figure 5), which is in agreement with increasing clay content (Table 3). The illuvial features described by micropedological observation are stress cutans (Table 7). We also detected the presence of zircon grains in P6, as indicated by the Zr and Si presence in the backscattered electrons images (Figure 5c).

Figure 6 shows higher amounts of K^+ in the inner K-feldspar grain, compared with the edge, and greater Na amount at the edge showing an intergrowth nature of Na-Plagioclase and K-Feldspar. The groundmass analysis indicates some Si losses (Figure 6). This is also observed in the Si/Al ratio, higher in the K-feldspar grain, reducing in the groundmass. Iron contents are higher in the micromass, with ferruginization of K-Feldspar grains at the edge, as hypocotings, and along fissures, as Fe-oxides infillings (Figure 6).

Table 7. Synthesis of the micropedology characteristics of the studied soils

Samples	Microstructure	Groundmass	C/F relative distribution	Organic materials	Pedofeatures
P1 Bhs (0.35-0.70 m)	Intergrain micro-aggregates and bridged grains, granular, very weak pedality, channels	Quartz coarse material, dark reddish-brown fine materials undifferentiated b-fabric	Enaulic and chitonic	Monomorphic OM, polymorphic material (pellety), decomposed OM fragments	Organic compound coatings, nodules, biologic channels
P2 C2 (0.70-0.90 m)	Bridged grains, granular, very weak pedality, channels	Quartz coarse material, dark reddish-brown fine materials, undifferentiated b-fabric	Enaulic	Monomorphic OM	Organic compound coatings, rare nodules
P5 C1 (0.08-0.20 m)	Pellicular and bridged grains, granular, weak pedality, simple packing voids	Quartz and feldspar coarse material, yellowish reddish-brown fine materials, undifferentiated b-fabric	Enaulic	Charcoal fragments	Clay coatings, nodules
P5 2C4 (1.00-1.10 m)	Massive, weak pedality, simple packing voids	Quartz and feldspar coarse material, yellowish reddish-brown fine materials, undifferentiated b-fabric	Chitonic	Not described	Nodules
P6 Bt1 (0.13-0.30 m)	Intergrain micro-aggregates, subangular blocks, weak/moderate pedality, channel and vesicular	Quartz coarse material, yellowish reddish-brown fine materials, undifferentiated b-fabric	Chitonic	Charcoal fragments	Clay coating, nodules
P6 Bt2 (0.30-0.55 m)	Intergrain micro-aggregates, subangular blocks, weak/moderate pedality, channel and vesicular	Quartz coarse material, yellowish reddish-brown fine materials, undifferentiated b-fabric	Chitonic	Not described	Clay coating, nodules
P6 Bt3 (0.55-1.00 m)	Intergrain micro-aggregates, subangular blocks, weak/moderate pedality, channel and vesicular	Quartz coarse material, yellowish reddish-brown fine materials, undifferentiated b-fabric	Chitonic	Not described	Clay coating, nodules
P7 2Bt (0.13-0.40 m)	Subangular blocky with strong coalescing, weak pedality, channel	yellowish, reddish fine materials, undifferentiated b-fabric	Porphyric	Not described	Clay coating, nodules
P8 Btv1 (0.85-1.10 m)	Subangular blocks, massive zones, very weak pedality, channel	yellowish reddish fine materials, undifferentiated b-fabric	Porphyric	Not described	Clay coating, nodules, iron coating

DISCUSSION

Podzolized soils of the Serra do Divisor

In the altitudinal sequence of Serra do Divisor, the migration of humic substances forming Fe and Al complexes is characteristic. Besides the sandstone geological substrate, which provides the coarser sandy texture, the high precipitation in this region also favors the podzolization process.

Our findings show nutrient-poor, dystrophic soils, with very low cation exchange capacity (CEC), high Al saturation, and low pH values on Serra do Divisor, which in agreement with previous results for other sandy soils studied in the Amazon (Lucas et al., 1993; Mafra et al., 2002; Gomes et al., 2007; Nascimento et al., 2008; Fritsch et al., 2009). However, the *Serra do Divisor* soils have some peculiar aspects, which result in much higher natural organic carbon accumulation than in other sandy soils of the Amazonia lowlands. In Serra do Divisor, this organic matter accumulation is due to the very low

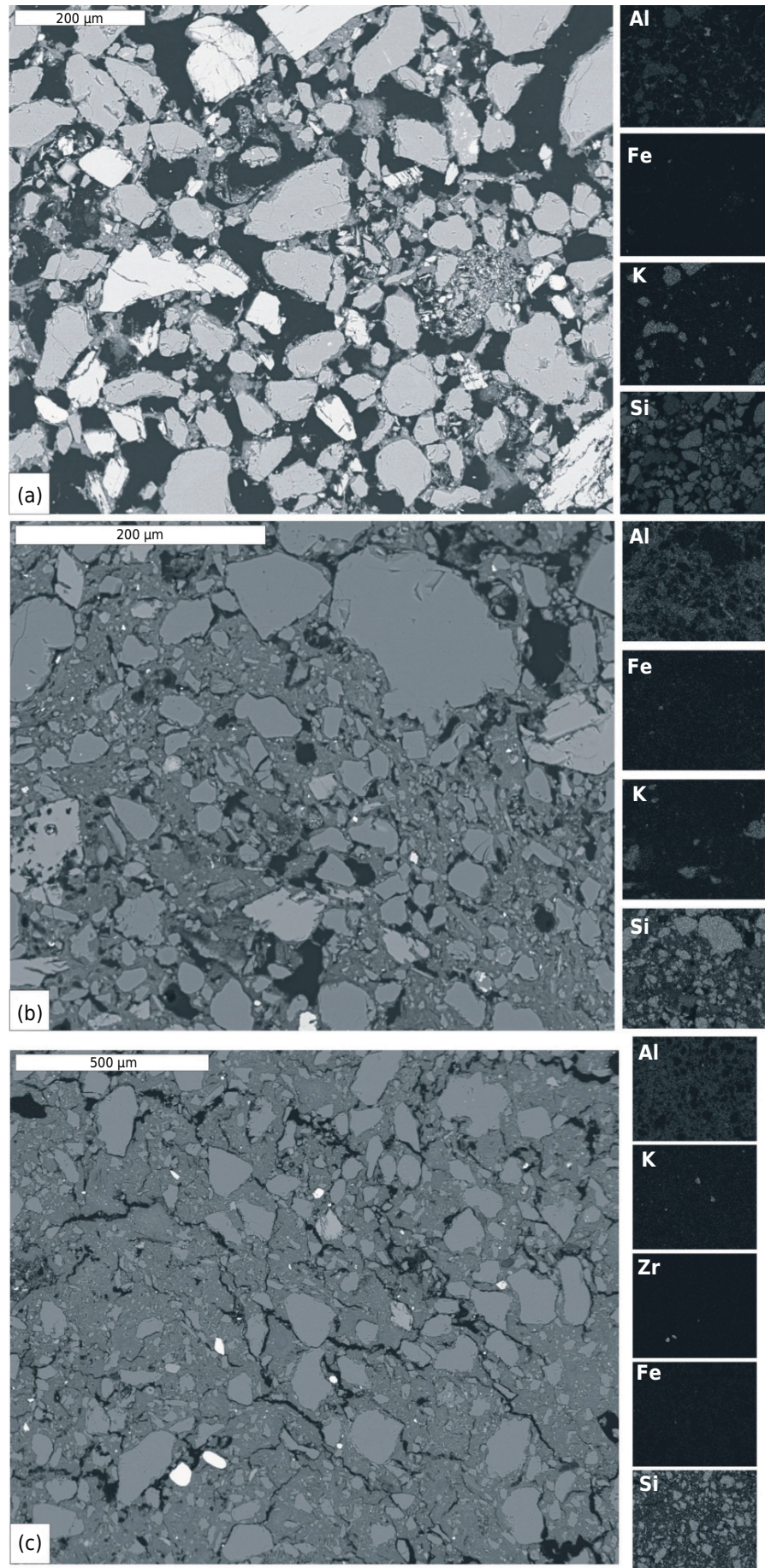


Figure 5. Backscattered electrons images and microchemical maps of soil horizons: (a) C1 of P5 with high porosity and (b) 2C4 horizon of P5 with higher clay content; and (c) Bt1 horizon of P6 with high clay content.

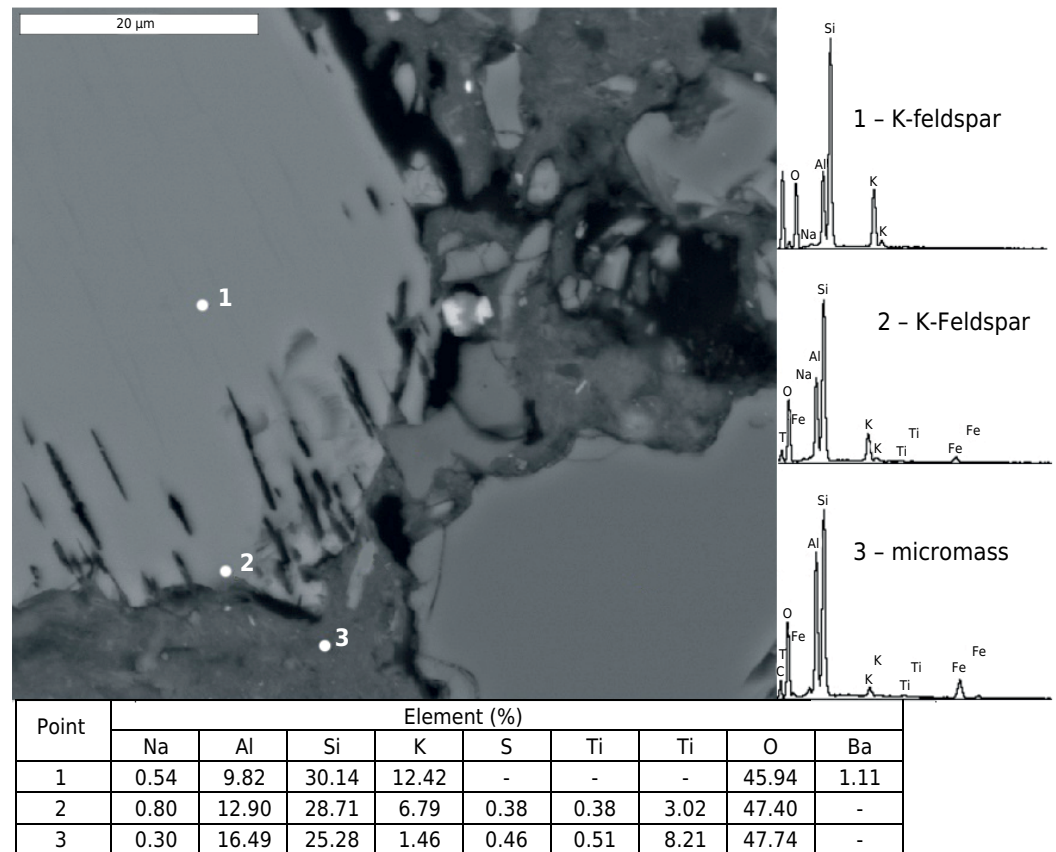


Figure 6. Detailed photomicrographs of Bt1 horizon of P6 with qualitative and quantitative EDS analyses: (1) K-feldspar; (2) K-feldspar; and (3) micromass.

nutrient status, high Al^{3+} levels and deposition of plant residues of slow decomposition rate, mostly dead leaves of *Bromeliaceae*, forming the understory stratum.

Organic matter (OM) associated with high Al levels have low biodegradation and high resistance to chemical oxidation (Mendonça, 1995). The predominance of H+Al, and particularly Al^{3+} in the exchange complex of the soils from Serra do Divisor, contributes to OM accumulation (Table 4), due to decreasing microbiological activity and accumulation of non-decomposed OM (Sieffermann et al., 1987). The strong nutrient depletion with depth in all soils, along with reduced TOC levels (Table 4), indicates the importance of surface OM for nutrient cycling in these chemically poor environments. Due to the sharp reduction of all nutrients with depth, Al^{3+} occupies most of the exchange complex in these sandy soils, with high organic matter mobility. In most soils, dissolved Al^{3+} can be leached from the topsoil (with $\text{pH} < 5$ in O and A horizons; Table 4) to the subsoil (with an increase in pH with depth; Table 4) during podzolization. Aluminum solubility increases sharply below pH 5 (McLean, 1976), and only precipitates as poorly crystalline Al hydroxides (e.g., imogolite) in the subsurface horizons with pH close to 5 (Table 4 and Figure 3).

Iron preferentially precipitates as ferrihydrite in soils with high organic carbon contents, in relation to goethite, hematite or lepidocrocite (Schwertmann et al., 1986). This is in agreement with the presence of ferrihydrite in the Bs and Bhs horizons at P1 at the highest location of Serra do Divisor.

The mountainous relief and high rainfall at Serra do Divisor enhance erosion and mass movement, which renews the landscape and exposes the weathered quartz-rich sediments, also nutrient-poor. These soils show high surface organic matter accumulation, whereas the coarse texture increases drainage and leaching, leaving

kaolinite and gibbsite as detrital minerals despite the quartzose substrate. This is consistent with studies from elsewhere in the Amazon (Bravard and Righi, 1988). However, the co-existence of gibbsite and kaolinite in the clay fraction in P1, with high TOC and low Prem (Table 4 and 5) in a predominantly quartz-sandy soil, indicates a possible in situ neof ormation of gibbsite, through biodegradation of organic matter complexed with Al (Volkoff et al., 1984; Bravard and Righi, 1988). The biogeochemical cycling of gibbsite is a possible mechanism in Podzols and the accumulation in deep horizons is not attributed to illuvial processes but to differential neof ormation between horizons with high and low organic matter contents (Vasquez, 1981). The crystallization of gibbsite in surface horizons is inhibited by the presence of organic matter (Wilson, 1969) and interaction with the organic matter may cause its re-dissolution to form highly stable organo-metallic complexes which are immobile due to their high content of complexed Al (Vasquez, 1981). Righi and DeConinck (1977) detected gibbsite in spodic horizons, suggesting in situ crystallization. The low Prem values at Bhs in P1 (Table 4) indicate the poorly crystalline Al/Fe phases (Table 5), with high P adsorption capacity (Novais and Smyth, 1999; Donagemma et al., 2008; Broggi et al., 2010).

The presence of imogolite was expected only in Bhs of P1, by the second one ratio, but this evidence must only be comproved by spectroscopy techniques. The imogolite genesis can be associated with Al-Si precipitated in the spodic horizons coming from O and E horizons, besides the participation of other minerals and humus accumulation can also be associated (Lundström et al., 2000). Normally, the imogolite is typical of Bs and C horizons of some Spodosols (Wada, 1989; Ugolini and Dahlgren, 1991). Some of the Al translocation occurs as “proto-imogolite” which might explain the presence of imogolite in the Bs horizons (Farmer and Lumsdon, 2001).

Moa river floodplain soils

The studied Alluvial soils were less influenced by carbonate-rich sediments (from the Ramon and Divisor Formations) upstream of Moa river or to rich clay of Solimões formation (Carvalho et al., 1977; Latrubesse et al., 2010), compared with the local Cretaceous sandstone. Hence, as evidenced by P5, the local erosion of the prominent Serra do Divisor leads to the deposition of sandy sediments, and formation of soils with high fine sand contents and with little contribution of the underlying Solimões formation.

Typic Kandiodults is the dominating soil developed on the Solimões Formation (Carvalho et al., 1977) and is represented in by P6, with the typical argillic horizon, and clay illuviation process. The lower nutrient availability with depth reflects the importance of vegetation in nutrient cycling and maintenance of higher bases saturation in surface horizons. However, clay illuviation and accumulation in depth in P7, is associated with high Ca^{2+} , forming an eutrophic argillic horizon. This high Ca^{2+} values can be explained by the influence of calcareous concretions in the Solimões formation in the local Cenozoic basin, as commonly found in Acre (Carvalho et al., 1977; Latrubesse et al., 2010). These results indicate a highly dynamic and complex environment, where deposition of alluvial or, and, colluvial material gives origin to soils with strong lithological variations. Our study shows significant changes in particle size distribution or mineralogy within a soil profile, like abrupt textural contacts, contrasting sand sizes, soil color, and micromorphological features, which indicate discontinuities (Soil Survey Staff, 2014).

The presence of plinthite in P8 (Btv1 horizon) indicates imperfect drainage and variations of water table depth, representing a limited zone for root and pedofauna development. The plinthite appears in a small amount in Btv1 horizon, without form a continuous phase, but indicates a plinthization process (Eze et al., 2014). This characteristic suggests an initial pedogenic process and changing drainage conditions.

The mineralogical aspects of the Moa river floodplain soils have some similarities to other soils from the Acre State. Gama (1986) studying soils developed on Plio-Pleistocenic sediments, elsewhere in Acre found chloritized minerals, mica, kaolinite, and quartz in the silt and clay fractions. Martins (1993) studying similar soils found kaolinite, montmorillonite, smectite with hydroxyl-Al interlayers, and muscovite. Mixing of materials, distinct depositional events and reworking of materials are possible explanations for the co-existence of such minerals in these soils.

All soils studied at the Moa river floodplain have clear redoximorphic processes, associated with water table variation, evidenced by the multicolored soil layers (Table 3). At the Moa river floodplain, all soils have layers with higher clay content and much lower Prem values than the upper layers, which we interpret as discontinuities and attribute the low Prem to the occurrence of Al and Fe oxides (gibbsite and goethite), probably with a detrital origin. The photomicrographs confirm the discontinuities, represented by differences in micromass content and c/f relative distribution (Table 7). The presence of zircon grains in P6 (Figure 5) indicates the mature detritic material of possible weathered quartz-rich Cretaceous sandstone, which influenced the fluvio-lacustrine deposits of Solimões formation (Kronberg et al., 1989; Horbe et al., 2019).

The dissolution features on feldspar grains suggest ongoing chemical weathering (Figure 6). The groundmass has no genetic relation to the K-feldspar, indicating a mixed sediment contribution (Solimões Formation). Dessilification process and enrichment of Fe hydroxides were detected in the P6 groundmass.

CONCLUSIONS

The highland *Serra do Divisor* soils have peculiar aspects with high natural organic carbon accumulation, in contrast with the low carbon contents of the adjacent Moa river floodplain soils. The Podzols have an accumulation of organic material in the surface horizons, attributed to the low nutrient status and high Al³⁺ levels and low decomposition. Kaolinite, quartz, and gibbsite coexist, and there is evidence of ferrihydrite and imogolite presence in these soils.





The coarse sandy nature of *Serra do Divisor* soils promote good drainage and leaching, forming detrital kaolinite and gibbsite but in situ neoformation of gibbsite, from the degradation of OM-Al compounds, is also possible.





At the Moa river floodplain, all soils are originated from Holocene sediments. Many contrasting soil processes were detected, like clay illuviation, sediment discontinuity, plinthization, and redoximorphism as dominants. These soils are generally richer in nutrients than those from the *Serra do Divisor*, have high Al³⁺ levels, and mixed mineralogy, with 2:1 clays, hydroxyl-Al interlayered smectite and kaolinite.



ACKNOWLEDGEMENTS




We thank the Protected Areas of Amazon Program (ARPA) and IBAMA/ICMBio Cruzeiro do Sul for financing and the logistics support during the expedition. Also, thanks CNPq and CAPES for the concession scholarships and the Unicamp for the photomicrographs and EDS analyses.



AUTHOR CONTRIBUTIONS





Conceptualization:  Bruno Araujo Furtado de Mendonça (lead),  Carlos Ernesto Gonçalves Reynaud Schaefer (lead),  Elpídio Inácio Fernandes-Filho (lead), and  Eufra Ferreira do Amaral (supporting).





Methodology:  Bruno Araujo Furtado de Mendonça (lead),  Carlos Ernesto Gonçalves Reynaud Schaefer (lead),  Elpídio Inácio Fernandes-Filho (lead), and  Felipe Nogueira Bello Simas (supporting).





Software:  Elpídio Inácio Fernandes-Filho (lead) and  Bruno Araujo Furtado de Mendonça (supporting).

Validation:  Bruno Araujo Furtado de Mendonça (lead),  Carlos Ernesto Gonçalves Reynaud Schaefer (supporting), and  Felipe Nogueira Bello Simas (supporting).

Formal analysis:  Bruno Araujo Furtado de Mendonça (lead) and  Felipe Nogueira Bello Simas (supporting).






Investigation:  Bruno Araujo Furtado de Mendonça (lead),  Carlos Ernesto Gonçalves Reynaud Schaefer (lead),  Elpídio Inácio Fernandes-Filho (lead), and  Felipe Nogueira Bello Simas (supporting).




Resources:  Elpídio Inácio Fernandes-Filho (lead),  Carlos Ernesto Gonçalves Reynaud Schaefer (lead),  Bruno Araujo Furtado de Mendonça (lead), and  Eufan Ferreira do Amaral (supporting).




Data curation:  Bruno Araujo Furtado de Mendonça (lead),  Carlos Ernesto Gonçalves Reynaud Schaefer (supporting),  Elpídio Inácio Fernandes-Filho (supporting), and  Felipe Nogueira Bello Simas (supporting).





Writing - original draft:  Bruno Araujo Furtado de Mendonça (lead),  Carlos Ernesto Gonçalves Reynaud Schaefer (lead),  Elpídio Inácio Fernandes-Filho (supporting), and  Felipe Nogueira Bello Simas (supporting).

Writing - review and editing:  Bruno Araujo Furtado de Mendonça (lead),  Carlos Ernesto Gonçalves Reynaud Schaefer (lead),  Elpídio Inácio Fernandes-Filho (supporting), and  Felipe Nogueira Bello Simas (supporting).

Visualization:  Bruno Araujo Furtado de Mendonça (lead),  Carlos Ernesto Gonçalves Reynaud Schaefer (supporting),  Elpídio Inácio Fernandes-Filho (supporting),  Felipe Nogueira Bello Simas (supporting), and  Eufan Ferreira do Amaral (supporting).

Supervision:  Bruno Araujo Furtado de Mendonça (lead),  Carlos Ernesto Gonçalves Reynaud Schaefer (lead), and  Elpídio Inácio Fernandes-Filho (lead).

Project administration:  Bruno Araujo Furtado de Mendonça (lead),  Carlos Ernesto Gonçalves Reynaud Schaefer (lead), and  Elpídio Inácio Fernandes-Filho (lead).

Funding acquisition:  Carlos Ernesto Gonçalves Reynaud Schaefer (lead),  Elpídio Inácio Fernandes-Filho (lead),  Bruno Araujo Furtado de Mendonça (supporting), and  Eufan Ferreira do Amaral (supporting).

REFERENCE

- Alvares CA, Stape JL, Sentelhas PC, Gonçalves JLM, Sparovek G. Köppen's climate classification map for Brazil. *Meteorol Z.* 2013;22:711-28. <https://doi.org/10.1127/0941-2948/2013/0507>
- Alvarez V VH, Novais RF, Dias LE, Oliveira JA. Determinação e uso do fósforo remanescente. *Bol Inf Soc Bras Cienc Solo.* 2000;25:27-32.
- Anderson HA, Berrow ML, Farmer VC, Hepburn A, Russell JD, Walker AD. A reassessment of podzol formation processes. *J Soil Sci.* 1982;33:125-36. <https://doi.org/10.1111/j.1365-2389.1982.tb01753.x>
- Andrade H, Schaefer CEGR, Demattê JLI, Andrade FV. Pedogeomorfologia e micropedologia de uma seqüência de Latossolo - Areia Quartzosa Hidromórfica sobre rochas cristalinas do Estado do Amazonas. *Geonomos.* 1997;5:55-66. <https://doi.org/10.18285/geonomos.v5i1.189>

- Bonifacio E, Santoni S, Celi L, Zanini E. Spodosol-Histosol evolution in the Krkonoše National Park (CZ). *Geoderma*. 2006;131:237-50. <https://doi.org/10.1016/j.geoderma.2005.03.023>
- Boulet R, Chauvel A, Lucas Y. Les systèmes de transformation en pédologie. In: Association Française pour l'Etude du Sol, editor. Livre Jubilaire du Cinquantenaire. Paris: AFES; 1984. p. 167-79.
- Bravard S, Righi D. Micromorphology of an Oxisol-Spodosol catena in Amazonia (Brazil). *Dev Soil Sci*. 1990;19:169-74. [https://doi.org/10.1016/S0166-2481\(08\)70327-1](https://doi.org/10.1016/S0166-2481(08)70327-1)
- Bravard S, Righi D. Characteristics of clays in an Oxisol-Spodosol toposequence in Amazonia (Brazil). *Clay Miner*. 1988;23:279-89. <https://doi.org/10.1180/claymin.1988.023.3.05>
- Brewer R. Fabric and mineral analysis of soil. New York: John Wiley & Sons; 1973.
- Broggi F, Oliveira AC, Freire FJ, Freire MBGS, Nascimento CWA. Adsorption and chemical extraction of phosphorus as a function of soil incubation time. *Rev Bras Eng Agr Amb*. 2010;14:32-8. <https://doi.org/10.1590/S1415-43662010000100005>
- Buurman P, van Reeuwijk LP. Allophane and the process of podzol formation - a critical note. *J Soil Sci*. 1984;35:447-52. <https://doi.org/10.1111/j.1365-2389.1984.tb00301.x>
- Carvalho AL, Neves ADS, Barbosa RCM, Viana CDB, Stange A, Amaral Filho ZP. Folhas SB/SC. 18 Javari/Contamana; Geologia, Geomorfologia, pedologia, vegetação e uso potencial da terra. Rio de Janeiro: Projeto RadamBrasil; 1977. (Levantamento de Recursos Naturais, 13).
- Chen P-Y. Table of key lines in X-ray powder diffraction patterns of minerals in clays and associated rocks. Indiana: Geological Survey Occasional Paper; 1977.
- Claessen MEC. Manual de métodos de análise de solo. 2. ed. Rio de Janeiro: Embrapa Solos; 1997.
- Climate-data.org. Clima Mâncio Lima; 2020 [cited 2020 Apr 21]. Available from: <https://pt.climate-data.org/america-do-sul/brasil/acre/mancio-lima-32414/?amp=true#climate-graph>
- Donagemma GK, Ruiz HA, Alvarez V VH, Ker JC, Fontes MPF. Fósforo remanescente em argila e silte retirados de Latossolos após pré-tratamentos na análise textural. *Rev Bras Cienc Solo*. 2008;32:1785-91. <https://doi.org/10.1590/S0100-06832008000400043>
- Dubroeuq D, Volkoff B. From Oxisols to Spodosols and Histosols: evolution of the soil mantles in the rio Negro basin (Amazonia). *Catena*. 1998;32:245-80. [https://doi.org/10.1016/S0341-8162\(98\)00045-9](https://doi.org/10.1016/S0341-8162(98)00045-9)
- Dubroeuq D, Volkoff B, Pedro G. La couverture pédologique du bouclier du nord de l'Amazonie (bassin du Haut rio Negro). Séquence évolutive des sols et son role dans l'aplanissement généralisé des zones tropicales perhumides. *C R Acad Sci*. 1991;312:663-71.
- Eze PN, Udeigwe TK, Meadows ME. Plinthite and its associated evolutionary forms in soils and landscapes: a review. *Pedosphere*. 2014;24:153-66. [https://doi.org/10.1016/s1002-0160\(14\)60002-3](https://doi.org/10.1016/s1002-0160(14)60002-3)
- Farmer VC, Lumsdon DG. Interactions of fulvic acid with aluminum and a proto-imogolite sol: the contribution of E-horizon eluates to podzolization. *Eur J Soil Sci*. 2001;52:177-88. <https://doi.org/10.1046/j.1365-2389.2001.00377.x>
- Farmer VC, Russell JD, Berrow ML. Imogolite and proto-imogolite allophane in spodic horizons: evidence for a mobile aluminium silicate complex in podzol formation. *J Soil Sci*. 1980;31:673-84. <https://doi.org/10.1111/j.1365-2389.1980.tb02113.x>
- Fritsch E, Allard TH, Benedetti MF, Bardy M, Nascimento NR do, Li Y, Calas G. Organic complexation and translocation of ferric iron in podzols of the Negro River watershed. Separation of secondary Fe species from Al species. *Geochim Cosmochim Acta*. 2009;73:1813-25. <https://doi.org/10.1016/j.gca.2009.01.008>
- Gama JRNF. Caracterização e formação de solos com argila de atividade alta do Estado do Acre. Itaguaí [tese] Seropédica: Universidade Federal Rural do Rio de Janeiro; 1986.
- Gomes FH, Torrado PV, Macias F, Gherardi B, Peres JLO. Solos sob vegetação de restinga na Ilha do Cardoso (SP). I - Caracterização e classificação. *Rev Bras Cienc Solo*. 2007;31:1563-80. <https://doi.org/10.1590/S0100-06832007000600033>

- Horbe AMC, Roddaz M, Gomes LB, Castro RT, Dantas EL, Carmo DA. Provenance of the Neogene sediments from the Solimões Formation (Solimões and Acre Basins), Brazil. *J S Am Earth Sci.* 2019;93:232-41. <https://doi.org/10.1016/j.jsames.2019.05.004>
- Instituto Brasileiro de Geografia e Estatística - IBGE. Projeto de proteção do meio ambiente e das comunidades indígenas: diagnóstico geoambiental e socioeconômico - Área de influência da BR-364 trecho RioBranco/Cruzeiro do Sul. Rio de Janeiro: IBGE/IPEA; 1994.
- Klinge H. Podzol soils in the Amazon basin. *Eur J Soil Sci.* 1965;16:95-103. <https://doi.org/10.1111/j.1365-2389.1965.tb01423.x>
- Kronberg BI, Franco JR, Benchimol RE, Hazenberg G, Doherty W, VanderVoet A. Geochemical variations in Solimões formation sediments (Acre basin, Western Amazonia). *Acta Amazon.* 1989;19:319-33. <https://doi.org/10.1590/1809-43921989191333>
- Lathrap DW. The upper Amazon, Ancient peoples and places. London: Thames and Hudson; 1970.
- Latrubesse EM, Cozzuol M, Silva-Caminha SAF, Rigsby CA, Absy ML, Jaramillo C. The Late Miocene paleogeography of the Amazon Basin and the evolution of the Amazon River system. *Earth-Sci Rev.* 2010;99:99-124. <https://doi.org/10.1016/j.earscirev.2010.02.005>
- Little IP. Mobile iron, aluminium and carbon in sandy coastal podzols of Fraser Island, Australia: a quantitative analysis. *Eur J Soil Sci.* 1986;37:439-54. <https://doi.org/10.1111/j.1365-2389.1986.tb00376.x>
- Lucas Y, Chauvel A, Boulet R, Ranzani G, Scatolini F. Transição Latossolos-podzóis sobre a formação Barreiras na região de Manaus, Amazônia. *Rev Bras Cienc Solo.* 1984;8:325-35.
- Lucas Y, Luizão FJ, Chauvel A, Rouiller J, Nahon D. The relation between biological activity of the rain forest and mineral composition of soils. *Science.* 1993;260:521-3. <https://doi.org/10.1126/science.260.5107.521>
- Lundström US, van Breemen N, Bain D. The podzolization process: a review. *Geoderma.* 2000;94:91-107. [https://doi.org/10.1016/S0016-7061\(99\)00036-1](https://doi.org/10.1016/S0016-7061(99)00036-1)
- Mafra AL, Miklós AAW, Volkoff B, Melfi AJ. Pedogênese numa seqüência Latossolo Espodossolo na região do Alto Rio Negro, Amazonas. *Rev Bras Cienc Solo.* 2002;26:381-94. <https://doi.org/10.1590/S0100-06832002000200012>
- Malcolm RL, Mccracken J. Canopy drip: a source of mobile soil organic matter for mobilization of iron and aluminum. *Soil Sci Soc Am Pro.* 1968;32:834-8. <https://doi.org/10.2136/sssaj1968.03615995003200060036x>
- Martins JS. Pedogênese de Podzólicos Vermelho-Amarelos do estado do Acre, Brasil. Belém: Faculdade de Ciências Agrárias do Pará [tese]. Belém: Faculdade de Ciências Agrárias do Pará; 1993.
- McClain ME, Richey JE, Brandes JA. Dissolved organic matter and terrestrial-lotic linkages in the central Amazon basin of Brazil. *Global Biochem Cy.* 1997;11:295-311. <https://doi.org/10.1029/97GB01056>
- Mckeague JA, Day JH. Dithionite and oxalate-extractable Fe and Al as aids in differentiating various classes of soils. *Can J Soil Sci.* 1966;46:13-22. <https://doi.org/10.4141/cjss66-003>
- McLean EO. Chemistry of soil aluminum. *Commun Soil Sci Plan.* 1976;7:619-36. <https://doi.org/10.1080/00103627609366672>
- Mehra JP, Jackson ML. Iron oxides removal from soils and clays by a dithionite-citrate-bicarbonate system buffered with sodium bicarbonate. *Clay Clay Miner.* 1960;7:317-27. <https://doi.org/10.1016/B978-0-08-009235-5.50026-7>
- Mendonça BAF, Simas FNB, Schaefer CEGR, Fernandes-Filho EI, Vale-Júnior JF, Mendonça JGF. Podzolized soils and paleoenvironmental implications of white-sand vegetation (Campinarana) in the Viruá National Park, Brazil. *Geoderma Regional.* 2014;2-3:9-20. <https://doi.org/10.1016/j.geodrs.2014.09.004>
- Mendonça ES. Oxidação da matéria orgânica e sua relação com diferentes formas de Alumínio de Latossolos. *Rev Bras Cienc Solo.* 1995;19:25-30.

- Mendonça ES, Matos ES. *Matéria orgânica do solo: métodos de análises*. Viçosa, MG: Universidade Federal de Viçosa; 2005.
- Moura P, Wanderley A. *Noroeste do Acre: reconhecimentos geológicos para petróleo*. Rio de Janeiro: Departamento Nacional de Produção Mineral; 1938.
- Nascimento NR, Fritsch E, Bueno GT, Bardy M, Grimaldi C, Melfi AJ. Podzolization as a deferralitization process: dynamics and chemistry of ground and surface waters in an Acrisol - Podzol sequence of the upper Amazon Basin. *Eur J Soil Sci*. 2008;59:911-24. <https://doi.org/10.1111/j.1365-2389.2008.01049.x>
- Novais RF, Smyth TJ. *Fósforo em solo e planta em condições tropicais*. Viçosa, MG: Universidade Federal de Viçosa; 1999.
- Patel-Sorrentin N, Lucas Y, Eyrolle F, Melfi AJ. Fe, Al and Si species and organic matter leached off a ferrallitic and podzolic soil system from Central Amazonia. *Geoderma*. 2007;137:444-54. <https://doi.org/10.1016/j.geoderma.2006.10.002>
- Paton TR. *The formation of soil material*. London: George Allen and Unwin; 1978.
- Righi D, De Coninck F. Mineralogic evolution in hydromorphic sandy soils and podzols in "Landes du Médoc", France. *Geoderma*. 1977;19:339-59. [https://doi.org/10.1016/0016-7061\(77\)90074-X](https://doi.org/10.1016/0016-7061(77)90074-X)
- Rossetti DF, Toledo PM, Góes AM. New geological framework for Western Amazonia (Brazil) and implications for biogeography and evolution. *Quaternary Res*. 2005;63:78-89. <https://doi.org/10.1016/j.yqres.2004.10.001>
- Ruiz HA. Incremento da exatidão da análise granulométrica do solo por meio da coleta da suspensão (silte + argila). *Rev Bras Cienc Solo*. 2005;29:297-300. <https://doi.org/10.1590/S0100-06832005000200015>.
- Santos RD, Lemos RC, Santos HG, Ker JC, Anjos LHC. *Manual de descrição e coleta de solo no campo*. 5. ed. rev ampl. Viçosa, MG: Sociedade Brasileira de Ciência de Solo; 2005.
- Santos HG, Jacomine PKT, Anjos LHC, Oliveira VA, Lumbreras JF, Coelho MR, Almeida JA, Araújo Filho JC, Oliveira JB, Cunha TJF. *Sistema brasileiro de classificação de solos*. 5. ed. rev. ampl. Brasília, DF: Embrapa; 2018.
- Schaefer CEGR. Clima e paleoclima do Acre: memórias e cenários da aridez quaternária na Amazônia e implicações pedológicas. In: Anjos LHC, Silva LM, Wadt PGS, Lumbreras JF, Pereira MG, editores. *Guia de campo da 9ª Reunião Brasileira de Classificação e Correlação de Solos*. Brasília: Embrapa; 2013. p. 59-79.
- Schaefer CEGR, Lima HN, Teixeira WG, Vale-Junior JF, Souza KW, Corrêia GR, Mendonça BAF, Amaral EF, Campos MCC, Ruivo MLP. Solos da região amazônica. In: Curi N, Ker JC, Novais RF, Vidal-Torrado P, Schaefer CEGR, editores. *Pedologia: solos dos biomas brasileiros*. Viçosa, MG: Sociedade Brasileira de Ciência do Solo; 2017. p. 111-75.
- Schaetzl R, Anderson S. *Soils: genesis and geomorphology*. United Kingdom: University Press, Cambridge; 2005.
- Schwertmann U, Cornell RM. *Iron oxides in the laboratory: preparation and characterization*. 2nd ed. New York: John Wiley & Sons; 2000.
- Schwertmann U, Kodama H, Fischer WR. Mutual interactions between organics and iron oxides. In: Huang PM, Schnitzer M, editors. *Interactions of soil minerals with natural organics and microbes*. 2nd ed. Madison: Soil Science Society of America; 1986. p. 223-50.
- Sieffermann G, Triutomo S, Sadelman MT, Kristijono A, Parhadimulyo SA. The peat genesis in the lowlands of Central Kalimantan province: the respective influence of podzolisation and bad drainage, the two main processes of peat genesis in Kalimantan. *Yogyakarta: Orstom*; 1987.
- Silveira M, Daly D. *Florística e botânica econômica do Acre - Relatório final (1993-1997)*. Rio Branco: Universidade Federal do Acre/The New York Botanical Garden; 1997.
- Soil Survey Staff. *Keys to soil taxonomy*. 12th ed. Washington, DC: United States Department of Agriculture, Natural Resources Conservation Service; 2014a.

- Soil Survey Staff. Kellogg soil survey laboratory methods manual. Lincoln: United States Department of Agriculture, Natural Resources Conservation Service; 2014b. (Soil Survey Investigations Report, 42).
- Sombroek WG. Amazon landforms and soils in relation to biological diversity. *Acta Amazon.* 2000;30:81-100. <https://doi.org/10.1590/1809-43922000301100>
- Sombroek WG. Amazon soils: a reconnaissance of the soils of the Brazilian Amazon [thesis]. Wageningen: Wageningen University; 1966.
- Sparks DL, Page AL, Helmke PA. Methods of soil analysis. Chemical methods. Part 3. Madison: Soil Science Society of America; 1996.
- Stoops G, Marcelino V, Mees F. Interpretation of micromorphological features of soils and regoliths. 2nd ed. Netherlands: Elsevier Science; 2018.
- Swift RS. Organic matter characterization. In: Sparks DL, Page AL, Helmke PA, editors. Methods of soil analysis. Chemical methods. Part 3. Madison: Soil Science Society of America; 1996. p. 1018-20.
- Ugolini FC, Dahlgren RA. Weathering environments and occurrence of imogolite/allophane in selected Andisols and Spodosols. *Soil Sci Soc Am J.* 1991;55:1166-71. <https://doi.org/10.2136/sssaj1991.03615995005500040045x>
- Vasquez FM. Formation of gibbsite in soils and saprolites of temperate-humid zones. *Clay Miner.* 1981;16:43-52. <https://doi.org/10.1180/claymin.1981.016.1.03>
- Volkoff B, Cerri CC, Melfi AJ. Húmus e mineralogia dos horizontes superficiais de três solos de campo de altitude dos estados de Minas Gerais, Paraná e Santa Catarina. *Rev Bras Cienc Solo.* 1984;8:277-83.
- Wada K. Allophane and imogolite. In: Dixon JB, Weed SB, editors. Minerals in soil environments, 2nd ed. Madison: Soil Science Society of America; 1989. p. 603-38.
- Wilson MJ. A gibbsitic soil derived from the weathering of an ultrabasic rock on the island of Rhum. *Scot J Geol.* 1969;5:81-9. <https://doi.org/10.1144/sjg05010081>
- Yeomans JC, Bremner JM. A rapid and precise method for routine determination of organic carbon in soil. *Commun Soil Sci Plant Anal.* 1988;19:1467-76. <https://doi.org/10.1080/00103628809368027>